

High Cytoplasmic and Membranous Versus Nuclear Talin-1 Expression Associated With Malignancy Potential and Determine Survival and Metastasis of Clear Cell Renal Cell Carcinoma

Leili Saeednejad Zanjani (✉ saeednejadleily@yahoo.com)

Iran University of Medical Sciences <https://orcid.org/0000-0002-5035-3766>

Somayeh Vafaei

Iran University of Medical Sciences

Maryam Abolhasani

Iran University of Medical Sciences

Fahimeh Fattahi

Iran University of Medical Sciences

Zahra Madjd

Iran University of Medical Sciences

Primary research

Keywords: Talin-1 protein, Bioinformatics analysis, Renal cell carcinoma (RCC), Clear cell RCC (ccRCC), Tissue microarray (TMA)

Posted Date: December 28th, 2020

DOI: <https://doi.org/10.21203/rs.3.rs-132677/v1>

License: © ⓘ This work is licensed under a Creative Commons Attribution 4.0 International License. [Read Full License](#)

Abstract

Background: Talin-1 as a cytoskeleton protein participates in cell migration and has an essential role in cell adhesion, proliferation, tumorigenesis, invasion, and metastasis in various types of malignancies.

Methods: Bioinformatics analysis has been performed by using protein-protein interaction network, analyses among PRIDE databases, and indicated that Talin-1 protein as a potential prognostic focal adhesion factor in renal cell carcinoma (RCC). We, therefore, examined the protein expression levels and prognostic significance of Talin-1 with clinical follow-up in a total of 269 formalin-fixed paraffin-embedded tissue specimens from three important subtypes of RCC undergone radical nephrectomy and 30 adjacent normal tissues in three levels including, membrane, cytoplasm, and nucleus using immunohistochemistry on tissue microarrays. Then, we used a combined analysis with B7-H3 to confirm that Talin-1 may be related to metastasis.

Results: The results showed that the expression of Talin-1 is significantly upregulated in most RCCs compared to adjacent normal tissues in protein levels. Further, there was a statistically significant difference between the membranous and cytoplasmic expression of Talin-1 and different subtypes of RCC ($P < 0.001$, $P = 0.003$, respectively). High membranous and cytoplasmic expression of Talin-1 was significantly associated with advanced nucleolar grade ($P < 0.001$, all), microvascular invasion ($P = 0.007$, $P = 0.004$), histological tumor necrosis ($P = 0.020$, $P = 0.018$), and invasion to Gerota's fascia ($P = 0.025$, $P = 0.050$) in clear cell RCC (ccRCC). In addition, high membranous and cytoplasmic expression of Talin-1 was associated with significantly poorer disease-specific survival (DSS) ($P = 0.043$, $P = 0.024$, respectively) and progression-free survival (PFS) ($P = 0.046$, only in cytoplasmic expression). The co-expression of cytoplasmic Talin-1^{High}/B7-H3^{High} was observed to be associated with more aggressive tumor behavior and metastasis. Moreover, increased cytoplasmic expression of Talin-1^{High}/B7-H3^{High} compared to the other phenotypes was associated with poor prognosis and progression of the disease in patients with distant metastasis.

Conclusion: Collectively, these observations indicate that Talin-1 is an important molecule involved in the spread and progression of ccRCC when expressed particularly in the cytoplasm and may serve as a novel prognostic biomarker in ccRCC if follow up time more prolonged.

Introduction

Renal cell carcinoma (RCC) is the most common type of kidney cancer found in adults. It represents approximately 3% of adult malignancies and 90–95% of all neoplasms arising from the kidney (1, 2). The RCC incidence rates have been increasing during the decade (3). According to the American Cancer Society, an estimated 73,750 new cases (45,520 in males and 28,230 in females) and 14,830 deaths (9,860 in males and 4,970 in females) from RCC will occur in 2020 (4). If cancer has not metastasized, the 5-year survival rate is 65–90%, but this is lowered considerably when cancer has spread so that the 5-year survival rates for patients with stage IV disease are less than 20% (5). Unfortunately, ~ 20–30% of RCC patients have distant metastasis at initial diagnosis. In addition, about 25–40% of RCCs would relapse and ultimately develop into metastatic disease after resection of the primary tumor (6). Moreover, increasing resistance to targeted therapies have been occurred in advanced RCC patients (7). Therefore, prognostic and predictive biomarkers will be an urgent requirement to assist in early diagnosis and identify novel therapeutic targets for RCC.

To date, several subtypes of RCC have been defined, of which clear cell RCC (ccRCC) is the most common subtype (75–80%), followed by papillary RCC (pRCC) 15%, and chromophobe RCC (chRCC) around 5% (8). In this study, we have focused on all these three important histological subtypes of RCC.

High throughput proteomics was introduced as an innovative novel approach that paves the way for cancer diagnostic or prognostic biomarker discovery (9). The advantages of these types of studies can be the identification of effective proteins with a different expression and cellular functions in the samples in various diseases (10). Although a high level of variance exists in proteomics data, network, and enrichment analysis explore the hub genes and their related biological significance

among results (11). In the present study, protein-protein interaction (PPI) network analysis was performed for proteomics data of available studies that had reported proteins with significant differential expression in RCC tissue samples compared to adjacent normal tissues. Enrichment analysis of hub genes was obtained for a better understanding of influential genes in the RCC network. It was found that TLN1 (Talin-1) is one of the hub genes that could be practical as a prognostic marker in renal cancer.

Talin-1 is a ubiquitous cytoskeleton-associated protein with a high-molecular-weight which has been shown to play an essential role in regulating the activity of the integrin family of cell adhesion proteins using coupling integrins to F-actin (12, 13). Also, Talin-1 is responsible for binding to critical adhesion molecules, including integrins, vinculin, actin, and other focal adhesion kinases (FAKs) and induce cell cytoskeletal remodeling. Therefore increased expression of Talin-1 could lead to the development of tumor and migration (14, 15). A number of studies have demonstrated that overexpression of Talin-1 was associated with advanced disease and reduced overall survival (OS) in patients, including oral squamous cell carcinoma (OSCC) (16), prostate cancer (17), colon cancer (18), and nasopharyngeal carcinoma (NPC) (19). To date, the expression levels and clinical significance of Talin-1 in the RCC tumors remain unclear. Thus, in the current study, to validate and confirm the Talin-1 protein obtained from the network analysis on results of proteomics studies in RCC samples, we have investigated the membranous, cytoplasmic, and nuclear expression levels of Talin-1 protein in three important subtypes of RCC from formalin-fixed paraffin-embedded (FFPE) tissue samples which assembled on tissue microarrays (TMAs) using the immunohistochemistry (IHC) technique. Then, we sought to determine the association between expression levels of Talin-1 protein at different intensities in the cell membrane, cytoplasm, and nucleus, and clinicopathological parameters, including nucleolar grade, tumor stage, microvascular invasion, and other important clinicopathological characteristics of RCC as well as survival outcomes. Finally, we used combined analysis with another marker of our previous study, namely B7-H3 (20) which is useful for predicting progression and metastasis in ccRCC to confirm that Talin-1 may be related to metastasis.

Methods

Data source and network analysis

Search on PRoteomics IDentifications database (PRIDE) (<https://www.ebi.ac.uk/pride/>) (21) from 2019 to 2020 led to identifying three RCC studies that each of them included the proteomics information of one of the RCC subtypes and adjacent normal tissues. The results of proteomics analysis were downloaded from the supplementary information of their published articles (22–24). Venn diagram analysis was performed to find common significant differential proteins in three subtypes of RCC by OriginPro 2019 (<https://www.originlab.com/2019>, OriginLab Corporation, Northampton, MA, USA). PPI network was constructed using stringapp (<https://string-db.org/>) (25) with medium confidence > 0.4 in Cytoscape (<https://cytoscape.org/>) (26). Hub genes were identified with the highest degree of connectivity of PPI network analysis (highest confidence > 0.9). Next, hub genes highly associated with cancer (P -value > 0.5).

In both Jensen (27) and DisGeNET RDF v7.0 (<https://academic.oup.com/nar/article/48/D1/D845/5611674>) (28), disease libraries on Enrichr (amp.pharm.mssm.edu/Enrichr/) (29) were selected as key genes of RCC network for subsequent analysis. Enrichment analysis was done with ClueGO plugin (<http://apps.cytoscape.org/apps/cluego>) (30) based on gene ontology (GO) (<http://geneontology.org/>) and pathways, including Kyoto Encyclopedia of Genes and Genomes (KEGG) (<https://www.genome.jp/kegg/>) (31), Reactome (<https://reactome.org/>) (32), and WikiPathways (<https://www.wikipathways.org/index.php/WikiPathways>) (33) for key genes. GO analysis was contained cellular component (CC), biological process (BP), and molecular function (MF) domains. Finally, one hub gene was selected for the evaluation of expression using the IHC method in RCC tissues. Also, protein expression level for the selected hub gene was considered in divers tumors on UALCAN database (<http://ualcan.path.uab.edu/>) which provides protein expression analysis option using data from Clinical Proteomic Tumor Analysis Consortium (CPTAC) (<https://proteomics.cancer.gov/programs/cptac>) (34).

Study population

Two hundred-ninety five FFPE tissues from RCC tumor specimen who underwent radical nephrectomy were collected from a major referral university-based urology–nephrology center, the Hasheminejad Hospital, in Tehran, Iran, during 2008–2015. It was confirmed that none of the patients had received radiotherapy or chemotherapy. Three important subtypes of RCC were comprised in this study including ccRCC, pRCC (type I & II), and chRCC. Hematoxylin and eosin (H&E) stained pathology slides and clinical and pathological information were obtained from medical archival records. The following variables were included age, gender, the maximum diameter of tumor size, nucleolar grade, tumor stage, microvascular invasion (MVI), lymph node invasion (LNI), renal vein invasion, histological tumor necrosis (TN), renal sinus fat, and renal sinus invasion, perirenal fat invasion, Gerota's fascia invasion, distant metastasis, and tumor recurrence.

Clinical follow-up was available for all patients until July 2015. Information of disease-specific survival (DSS) was defined as the time from the first operation to death due to renal cancer. Progression-free survival (PFS) was defined as the interval between primary operation and the last follow-up visit without any disease, evidence of tumor recurrence, or metastasis. In addition, tumor stage and nucleolar grade were defined according to the pTNM classification for RCC (35–37). Moreover, it was agreed that chRCC should not be graded (36).

Tissue microarray (TMA) construction

The tissue samples were brought into a TMA format as follow, briefly, H & E slides were examined and the most representative areas of the tumor were marked by pathologists. 0.6-mm tissue cylinders were punched out from the selected regions of each donor tumor tissue blocks and transferred into a recipient paraffin block using tissue arrayer MiniCore (ALPHELYS, Plaisir, France). The TMA blocks were constructed in triplicate for each specimen. The mean of the three scores was calculated as the final score. Previous studies have shown that three cores are highly representative of the whole sections (38, 39). Finally, 4-µm sections were cut from array blocks and transferred to adhesive slides. In each TMA block, adjacent normal renal tissue samples (totally, 30 samples) were included to compare the expression pattern of Talin-1 protein compared to the tumor tissue samples.

Immunohistochemistry (IHC) for Talin-1 protein expression

IHC was applied to detect the expression of Talin-1 protein. Briefly, all TMA sections were deparaffinized at 60°C for 20 min and were transferred in xylene and rehydrated via a series of graded alcohols. 3% H₂O₂ was used to block endogenous peroxides and non-reactive staining for 20 min at room temperature. Antigen retrieval was performed by immersing the tissues in citrate buffer (pH 6.0) for 10 min in an autoclave. Sections were then incubated with a primary rabbit polyclonal antibody to Talin-1 (1:100, ab71333, Abcam Inc., Cambridge, MA, UK) at 4°C overnight. For isotype control, rabbit immunoglobulin G (IgG) (1:100, Invitrogen, Thermo Fisher Scientific, USA) was used. Then, TMA slides were incubated with anti-rabbit/anti-mouse Envision (Dako, Glostrup, Denmark) as a secondary antibody for 30 min. Afterward, the sections were visualized by diaminobenzidine (DAB) (Dako, Glostrup, Denmark) and stained with hematoxylin (Dako, Glostrup, Denmark). Finally, the slides were dehydrated in alcohol, cleared in xylene, and mounted for examination. In each run of the experiment, human normal kidney tissue was used as a positive control and replacement of the primary antibody with Tris-buffered saline (TBS) as a negative control to confirm the nonspecific bindings of the secondary antibody.

Immunohistochemistry evaluation

The evaluation procedure of the IHC was reviewed by one independent pathologist (M.A) without any related clinical data-informed. The intensity and percentage of the staining area were considered as two important components of the scoring system for Talin-1 protein expression. The intensity of staining was scored by applying a semi-quantitative system, ranging from negative to strong as follows: 0 (no staining), 1 (weak), 2 (moderate), and 3 (strong). The percentage of staining area was categorized according to the positive tumor cells: less than 25% positive cells, 25–50% positive cells, 51–75% positive cells, and more than 75% positive cells. The final Talin-1 protein expression score was calculated by multiplying the value of the intensity score by the percentage of positive tumor cells which ranged from 0 to 300, namely histochemical score (H-score). In this study, the median H-score was chosen to categorize samples with high or low Talin-1 protein expression.

Combined analysis of Talin-1/B7-H3 markers

Previous studies have shown that an association between increased expression of B7-H3 and potential to metastasize (20, 40), therefore we applied our previous data of B7-H3 in ccRCC (20) to used combined analysis to confirm that Talin-1 may be related to metastasis.

Statistical analysis

Analyses were performed using the “statistical software SPSS, version 22.0. Armonk, NY: IBM Corp”. To verify the significance of association and correlation between Talin-1 protein expression and clinicopathological parameters, Pearson's chi-square and Spearman's correlation tests were performed. Kruskal-Wallis and Mann-Whitney *U* tests were applied for pairwise comparison between groups. Survival curves by Talin-1 status were estimated using the Kaplan–Meier method with 95% confidence interval (CI) and compared by the log-rank test. Univariate Cox proportional hazard models were fit to identify factors significantly related to DSS or PFS. To assess whether Talin-1 and the other variables were an independent predictor of survival, multivariate Cox models were also assessed. The data were expressed as the mean; standard deviation (SD) and median; quartile (Q1, Q3). The difference was considered statistically significant at a *P*-value < 0.05.

Results

Bioinformatics approach

Significant differential expression of proteins from tumor tissues in comparison to adjacent normal tissues was obtained of selected previous studies that include 1055, 589, and 983 proteins for ccRCC, pRCC, and chRCC, respectively (Supplementary Table 1). The results of the Venn diagram analysis illustrated 110 common differential expression proteins between subtypes of RCC (Fig. 1). PPI network analysis result explored 52 hub genes with the highest confidence > 0.9 (Fig. 2) that 24 key genes have reported for cancer on both Jensen and DisGeNET databases (Supplementary Table 1). Pathway analysis displays that most key genes contribute to metabolism pathways and several genes involved in FAK and degradation of extracellular matrix (ECM) pathways (Fig. 3). The major part of GO analysis results for 24 key genes indicates these genes are present in the microbody and play role in fatty acid catabolic process. Also, the basement membrane organization is a remarkable part of gene annotation results (Supplementary Fig. 1). According to these results, key genes involved in FAK and pathways related to ECM, as key drivers for both development and cancer progression (41), were highlighted for selection marker. Our key genes list, including COL4A1, LAMB2, NID1, and TLN1 (Talin-1) were evaluated among literature and led to the selection of Talin-1 as our final biomarker for investigation in RCC. Talin-1 as a master integrin-associated protein is a focal adhesion (FK) complex that mediates ECM proteolysis through different matrix metalloproteinases (MMPs) expression (42). FAK activation triggers the following processes, including survival, angiogenesis, cell growth, migration, and invasion. Since FAK functions potentially regulate gene expression to affect cancer progression (43), it seems that its signaling to be vital in the neoplastic cells invasion, and its activity inhibition decrease RCC metastasis both *in vitro* and *in vivo* (44–46). Although the FAK signaling pathway is deregulated in different cancer types and its importance approved in the regulation of cell adhesion and motility due to the tumor invasive behavior (47–49), its evidence in RCC is few and it is necessary to explore which is crucial (42). Further, UALCAN database revealed a higher expression of Talin-1 protein in ccRCC tissue samples compared to normal samples (Fig. 4).

Characteristics of RCC patients

Two hundred and ninety-five RCC patients were included in this study, while technical problems led to a loss of some cases, and finally, 269 cases remained for evaluating. These samples include 195 (73.58%) ccRCC, 20 (7.43%) pRCC type I, 20 (7.43%) pRCC type II, and 34 (12.63%) chRCCs. The patients' clinicopathological characteristics were summarized in Table 1 based on whole RCC samples and histological subtypes of RCC.

Expression of Talin-1 protein in the subtypes of RCC and adjacent normal tissue samples

The expression level of Talin-1 protein was evaluated using the IHC method on TMA sections by three scoring methods, including the intensity of staining, percentage of positive tumor cells, and H-score in histological subtypes of RCC and adjacent normal tissue samples. Talin-1 protein was expressed at different intensities in the cell membrane, cytoplasm, and nucleus in the samples (Table 2) (Fig. 5), however, the expression of Talin-1 protein in adjacent normal tissue samples was less compared to tumor samples.

Comparison of Talin-1 protein expression based on histological subtypes of RCC

In this part of the study, to compare differences between the median expression levels of Talin-1 protein in the membrane, cytoplasm, and nucleus among the histological subtypes of RCC, the non-parametric Kruskal–Wallis and Mann–Whitney *U* tests were applied. The results of the Kruskal–Wallis test revealed a statistically significant difference between the membranous and cytoplasmic Talin-1 protein expression levels in different RCC subtypes ($P < 0.001$, $P = 0.003$, respectively). Also, Mann–Whitney *U* test showed a statistically significant difference in the median levels of membranous and cytoplasmic Talin-1 protein expression between ccRCC and pRCC (type I & II) ($P < 0.001$, $P = 0.001$, respectively) and also pRCC (type I & II) and chRCC ($P = 0.006$, $P = 0.029$, respectively) (Fig. 6A, B). In contrast, the Kruskal-Wallis test showed that there is no statistically significant difference between the median expression level of nuclear Talin-1 protein in different subtypes of RCC ($P = 0.904$) (Table 3). Moreover, we did not find a statistically significant difference in the median expression level of nuclear Talin-1 protein between the RCC subtypes (Fig. 6C).

Associations between membranous, cytoplasmic, and nuclear Talin-1 protein expression and clinicopathological parameters in histological subtypes of RCC

ccRCC:

In ccRCC, membranous and cytoplasmic expression of Talin-1 protein were observed in 195 (100.0%) patients and nuclear Talin-1 expression in 180 (92.3%) cases.

Pearson's chi-square test was used to examine the association between Talin-1 protein expression and clinicopathological parameters in histological RCC subtypes. The results of Pearson's chi-square test showed a highly significant association between expression of membranous and cytoplasmic Talin-1 protein and increased nucleolar grades (I + II versus III + IV) (Pearson's chi-square, $P < 0.001$, all) (Table 4). Kruskal–Wallis and Mann–Whitney *U* tests also showed that statistically significant differences in the median levels of membranous and cytoplasmic Talin-1 protein expression in various nucleolar grades ($P = 0.001$, $P < 0.001$, respectively) (Fig. 7A, B). Moreover, Pearson's chi-square test revealed that significant differences between higher levels of expression of membranous and cytoplasmic Talin-1 protein and MVI ($P = 0.007$, $P = 0.004$, respectively), histological TN ($P = 0.020$, $P = 0.018$, respectively) as well as Gerota's fascia invasion ($P = 0.025$, $P = 0.050$, respectively). Furthermore, there was a statistically significant difference between higher level of membranous Talin-1 protein expression and invasion to renal pelvis ($P = 0.038$). Kruskal–Wallis and Mann–Whitney *U* tests also indicated a statistically significant difference between the median expression levels of membranous and cytoplasmic Talin-1 protein and MVI ($P = 0.022$, $P = 0.007$, respectively) (Fig. 7C, D). Bivariate analysis (Spearman's correlation) showed a significant direct correlation between membranous and cytoplasmic expression and advanced in nucleolar grades (Spearman's rho, $P < 0.001$, $P = 0.001$, respectively), MVI ($P = 0.007$, $P = 0.004$, respectively), histological TN ($P = 0.015$, $P = 0.014$, respectively), and invasion to Gerota's fascia ($P = 0.025$, $P = 0.050$, respectively). The results of Spearman's correlation analysis also revealed that membranous Talin-1 protein expression and renal pelvis ($P = 0.038$) were directly correlated. In this study, we did not find any significant association and correlation between nuclear Talin-1 protein expression and clinicopathological features in ccRCC cases (Table 4).

pRCC (type I & II) and chRCC:

Membranous and cytoplasmic expression of Talin-1 protein was observed in all cases 20 (100.0%), 20 (100.0%), and nuclear Talin-1 expression in 11 (55.0%), 12 (60.0%) patients of pRCC type I and pRCC type II, respectively. In the cases of chRCC, membranous and cytoplasmic Talin-1 protein expression were found in 34 (100.0%) patients and nuclear expression in 25 (73.5%) cases. The results of Pearson's chi-square and Spearman's correlation tests revealed that there are no significant association and correlation between membranous, cytoplasmic, and nuclear Talin-1 protein expression and clinicopathological parameters in pRCC (type I & II) (Tables 5, 6). In chRCC, we observed a statistically significant association between membranous expression of Talin-1 and tumor stage ($P = 0.050$) (Table 7). Moreover, Spearman's correlation analysis showed a statistically significant positive correlation between increased Talin-1 protein expression and higher tumor stage (Spearman's rho, $P = 0.023$).

Prognostic value of expression of Talin-1 protein for clinical outcomes in histological subtypes of RCC

In the current study, the mean and median duration of the follow-up time for DSS were 52 (SD = 27.5) months and 49 (Q1, Q3 = 34, 71) and for PFS were 49 (SD = 29.6) and 47 (Q1, Q3 = 31, 71) months, respectively. Also, the minimum and maximum of follow-up time were 1 and 117 months and the range was 116 months. The results of the analysis showed that distant metastasis and tumor recurrence occurred in 55 (20.4%) and 41 (15.2%) patients, respectively whereas, 214 (79.6%) and 228 (84.8%) were not positive for mentioned parameters. Also, 63 (23.4%) patients were positive for distant metastasis or tumor recurrence and 206 (76.6%) were not positive for these features. During the follow-up, cancer-related death occurred in 40 patients (14.9%) and disease-related death in 5 (1.9%). The main characteristics of patients enrolled for survival analysis according to the histological subtypes of RCC were summarized in (Table 8).

Survival outcomes based on the expression of Talin-1 protein in the histological subtypes of RCC

The association between expression of membranous, cytoplasmic, and nuclear Talin-1 protein and DSS or PFS were evaluated using Kaplan–Meier analysis curves and the log-rank test.

ccRCC:

Survival outcomes based on membranous Talin-1 protein expression

The results of the Kaplan–Meier curve demonstrated that significant differences between DSS and the patients with high and low membranous expression of Talin-1 protein (Log-rank test: $P = 0.043$) (Fig. 8A). The mean DSS time for patients with high and low membranous expression of Talin-1 protein was 91 (SD = 4.6) and 103 (SD = 3.5) months, respectively. Additionally, the 5-year survival rates for DSS in patients whose specimens expressed high and low membranous expression of Talin-1 protein were 78 and 88%, respectively (Log-rank test: $P = 0.050$). Moreover, the results of the Kaplan–Meier analysis for PFS showed that there are no significant differences between PFS and the patients with high and low expression of membranous Talin-1 protein (Log-rank test: $P = 0.081$) (Fig. 8B).

Survival outcomes based on cytoplasmic Talin-1 protein expression

Our finding of Kaplan–Meier curves analysis in the cytoplasmic expression of Talin-1 revealed that significant differences between DSS (Log-rank test: $P = 0.024$) or PFS (Log-rank test: $P = 0.046$) and the patients with high and low cytoplasmic Talin-1 protein expression, respectively (Fig. 8C, D). Further, the mean DSS or PFS time for patients with high and low cytoplasmic expression of Talin-1 protein were 90 (SD = 4.7), 87 (SD = 5.0) and 103 (SD = 3.4), 99 (SD = 3.9) months, respectively. The 5-year survival rates for DSS or PFS of patients with high cytoplasmic Talin-1 protein expression were 77 and 72% and with low expression were 89 and 85% (Log-rank test: $P = 0.044$, $P = 0.050$, respectively).

Survival outcomes based on nuclear Talin-1 protein expression

Kaplan Meier survival curves showed that there are no significant differences between DSS or PFS and the patients with high and low nuclear expression of Talin-1 protein in ccRCC cases (Log-rank test: $P = 0.160$, $P = 0.219$, respectively) (Fig. 9A, B).

Our finding from univariate analysis showed that the membranous and cytoplasmic expression of Talin-1 protein ($P = 0.048$, $P = 0.028$, respectively), tumor size ($P = 0.009$), nucleolar grade ($P < 0.001$), and tumor stage ($P = 0.029$) were significant risk factors affecting the DSS with hazard ratio (HR) more than 1 and cytoplasmic expression of Talin-1 protein ($P = 0.050$), tumor size ($P = 0.004$), nucleolar grade ($P < 0.001$), and tumor stage ($P = 0.047$) were significant risk factors affecting the PFS of patients with ccRCC (Tables 9, 10). As demonstrated in Tables 9 and 10, nucleolar grade was the only independent prognostic factor for DSS (membranous expression; HR: 2.563, 95% CI: 1.119–5.869; $P = 0.026$, cytoplasmic expression; HR: 2.483, 95% CI: 1.095–5.633; $P = 0.029$) or PFS (cytoplasmic expression; HR: 2.243, 95% CI: 1.061–4.739; $P = 0.034$) in the multivariate analysis. Expression of membranous and cytoplasmic Talin-1 protein for DSS ($P = 0.356$, $P = 0.219$, respectively) and cytoplasmic expression of Talin-1 for PFS ($P = 0.312$) were not significant risk factors for prognosis in the multivariate analysis (Tables 9, 10). Other clinicopathologic variables were not significant factors affecting the DSS or PFS in univariate and multivariate analyses of ccRCC patients.

pRCC (type I & II) and chRCC:

Kaplan–Meier survival analysis showed that there is no statistically significant association between membranous, cytoplasmic, and nuclear Talin-1 protein expression and patients' survival outcomes in pRCC (type I & II) and chRCC patients. Additionally, univariate and multivariate analyses demonstrated that the listed clinicopathologic variables are not significant factors affecting the DSS or PFS of patients with papillary and chRCC.

Combined analysis of Talin-1/B7-H3 populations

In this part of the study, we first chose the samples which have stained in two markers, thus the number of patients was 138. The results showed that a statistically significant correlation between expression of cytoplasmic Talin-1 and cytoplasmic B7-H3 proteins (Spearman's rho, 0.318; $P < 0.001$), however, in membranous expression, we did not find any significant correlation between two markers (Spearman's rho, 0.026; $P = 0.756$). Therefore, we examined the association between co-expression of cytoplasmic Talin-1 and cytoplasmic B7-H3 proteins with clinicopathologic parameters. The expression levels of Talin-1 and B7-H3 were divided into two categories based on median expression and four phenotypes including Talin-1^{High}/B7-H3^{High}, Talin-1^{High}/B7-H3^{Low}, Talin-1^{Low}/B7-H3^{High}, and Talin-1^{Low}/B7-H3^{Low} (Table 11). The analysis showed that a highly significant association between cytoplasmic Talin-1^{High}/B7-H3^{High} phenotype and nucleolar grade ($P = 0.002$). The cytoplasmic Talin-1^{High}/B7-H3^{High} phenotype was more often found in patients with MVI present ($P = 0.002$), histological TN present ($P = 0.026$), Gerota's fascia invasion ($P = 0.043$), and distant metastasis ($P = 0.022$) compared to patients without MVI and histological TN, as well as no invasion to Gerota's fascia and no distant metastasis (Table 11).

Survival outcomes of Talin-1/B7-H3 expressions

The survival rate of patients with co-expression of cytoplasmic Talin-1^{High}/B7-H3^{High} phenotype was compared with other phenotypes. Higher cytoplasmic expression of Talin-1^{High}/B7-H3^{High} phenotype was associated with worse DSS and PFS than another phenotype (Log-rank test; $P = 0.007$, $P = 0.021$, respectively) (Fig. 10A, B). Further, the 5-year survival rates for DSS and PFS were 87.0% and 83.0% in cytoplasmic Talin-1^{High}/B7-H3^{High} phenotype expression, and 67.0% and 65.0% in another phenotype of cytoplasmic Talin-1/B7-H3 expression (Log-rank test; $P = 0.010$, $P = 0.029$, respectively). Moreover, the stratified analysis indicated that in the patients with distant metastasis, the differences in DSS between patients with cytoplasmic Talin-1^{High}/B7-H3^{High} phenotype and other phenotypes of Talin-1/B7-H3 expression is significant ($P = 0.050$) (Fig. 10C, D).

Tumor size (10.1 cm versus < 4 cm) and nucleolar grade were the significant risk factors affecting the DSS or PFS of patients with ccRCC in univariate analysis, with hazard ratios of 6.476, 4.338 and 6.737, 3.418 and P values of 0.016, 0.001, and 0.013, 0.001, respectively.

Discussion

Although much progress has been made big changes in the treatment of RCC, drug resistance to targeted therapies brings more failures in advanced RCC patients' treatment (7). Thus, it is urgently needed to explore novel and practical clinical prognostic markers of RCC in the patient's early diagnosis in future renal cancer therapy.

The bioinformatics analysis would be conducive to molecular markers research in clinical RCC. This study set out with the aim to identify the novel biomarker that was potentially involved in the various RCC subtypes. In this regard, we focused on PPI network analysis for proteomics results of other studies related to RCC subtypes and used bioinformatics software investigations to identify hub genes. The hub genes were generated based on the highest degree of connectivity and were screened on Enricher for cancer disease. Besides, enrichment analysis determined the involved pathways and molecular function of hub genes. These results suggested several proteins as hub genes related to cancer, which among them we selected Talin-1 and warranted further investigation. Therefore, to validate the Talin-1 protein as a prognostic marker for RCC, for the first time, expression levels of Talin-1 protein was investigated in a well-characterized series of 269 tissues specimen from patients treated with radical nephrectomy in three main subtypes of RCC including 195 (73.58%) ccRCC, 20 (7.43%) pRCC type I, 20 (7.43%) pRCC type II, and 34 (12.63%) chRCC tissue samples through IHC on TMA slides and evaluation of the association between its expression and clinicopathological characteristics as well as patient survival outcomes. The pattern of Talin-1 protein expression in RCCs also was classified into membranous, cytoplasmic, and nuclear expression.

It is important to investigate histological subtypes of specific cancer, giving consideration to various subtypes which may be associated with different biologic behavior, pattern, and prognosis, hence each of them needs different treatment. The evaluation of the staining pattern in each subtype of RCC displayed differential expression of Talin-1 protein in membrane, cytoplasm, and nucleus with a range of intensities from weak to strong as well as the percentage of staining area. Further, there was a statistically significant association between the membranous and cytoplasmic expression of Talin-1 protein but not in nuclear expression and the RCC subtypes. Subsequently, a statistically significant difference was observed in the median levels of membranous and cytoplasmic Talin-1 protein expression between ccRCC and pRCC (type I & II) ($P < 0.001$, $P = 0.001$, respectively) as well as pRCC (type I & II) and chRCC subtype ($P = 0.006$, $P = 0.029$, respectively), indicating that expression of Talin-1 protein in membrane and cytoplasm versus nucleus are more important in subtypes of RCC and also these expression patterns vary among the histological RCC subtypes, thus this may affect on the prognostic value of them and ways to treat of patients.

IHC analysis of human RCCs compared to adjacent normal tissue samples demonstrated that Talin-1 protein expression is upregulated in RCCs. The present study also considered the expression of Talin-1 on UALCAN database, containing a large amount of proteomics data which showed that increased expression of Talin-1 in ccRCCs rather than normal samples. Thus, these results are in line with our findings of Talin-1 protein expression using IHC on ccRCCs.

The advantage of analyzing the expression and subcellular distribution of Talin-1 in RCCs is, the protein in different subcellular localization may have a specific function. Our finding showed that membranous and cytoplasmic expression of Talin-1 protein is positively associated with the important clinicopathological parameters, including advanced nucleolar grade, MVI, histological TN, invasion to Gerota's fascia, and renal pelvis, while in nuclear expression, there was no any association between expression of Talin-1 protein and clinicopathological features in ccRCC cases. Importantly, our results exhibited the increased expression of the median membranous and cytoplasmic of Talin-1 protein in the high grade of RCC (nucleolar grade III + IV) compared with the low grade of RCC (nucleolar grade I + II) and also increased expression in patients with MVI present rather than MVI absent which exhibited the association of membranous and cytoplasmic Talin-1 protein expression with the aggressiveness of ccRCC. In addition, in this study nucleolar grade was found as an independent prognostic factor for DSS and PFS in membranous and cytoplasmic Talin-1 protein expression in multivariate analysis. After the tumor stage, one the strongest prognosticators of survival in patients with RCC is the nucleolar grade, and tumors with a high nucleolar grade display a more aggressive phenotype; thus they are associated with local invasion and distant metastasis (50). Previous studies demonstrated that MVI is related to cancer progression and survival in RCC and is the most

significant prognostic variable for prognostication of metastatic spread and survival outcome independent from macrovascular invasion (51, 52). Histological TN also has proposed to be a sign of tumor aggressiveness that generally leads to poor survival outcomes (53). A recently systematic review and meta-analysis study suggested that histological TN is associated with DSS, OS, RFS (recurrence-free survival), and PFS of RCC patients and may serve as a predictor of poor prognosis in RCC patients (54). Moreover, in this study tumor size and tumor stage were found as prognostic variables in univariate analysis that depicted the associations between these parameters and more aggressive tumor behaviors. The tumor stage is one of the most factors for predicting tumor progression and recurrence in RCC (55) and tumor size has shown significantly associated with the risk of metastasis (56). Therefore, these results indicated that membranous and cytoplasmic Talin-1 protein expression compared with nuclear expression are related to the degree of malignancy and progression of disease in ccRCC cases.

Our results from Kaplan-Meier survival curves in ccRCC cases showed that higher membranous and cytoplasmic Talin-1 protein expression is associated with significantly worsened DSS as well as worsened DSS or PFS compared to low Talin-1 protein expression, respectively. In addition, ccRCC patients, who expressed a high level of membranous and cytoplasmic Talin-1, had shorter 5-year DSS or PFS compared with those with low expression. However, the pattern of Talin-1 protein expression was not a predictor of survival in multivariate analysis, indicating the long term follow-up is needed to increase the events and prognosis.

Investigations have shown that increased expression of Talin-1 could lead to the progression of tumor cell adhesion and migration because of Talin-1 as a FA protein is able to mediate integrin interaction with ECM and can bind to a variety of adhesion molecules and induce cell cytoskeleton remodeling (23). B7-H3, also a member of the B7 family of immunoregulatory proteins which is overexpressed in many types of malignancies and is linked to poor prognosis, increased tumor grade, and metastasis (57). Previous studies have been reported a correlation between expression levels of B7-H3 and progression of disease in ccRCC (20, 58). To confirm that whether Talin-1 is related to metastasis, we used the combined analysis of both Talin-1 protein and our previous data of B7-H3 protein in ccRCC. The co-expression of cytoplasmic Talin-1^{High}/B7-H3^{High} was observed to be associated with more aggressive tumor behavior and metastasis. Further, Tumor size and nucleolar grade were the significant risk factors affecting the DSS or PFS which depict tumor aggressiveness. Moreover, increased cytoplasmic expression of Talin-1^{High}/B7-H3^{High} compared to the other phenotypes was associated with poor prognosis and progression of the disease, especially in patients with distant metastasis, therefore, our findings revealed that increased cytoplasmic expression of Talin-1 is associated with invasiveness and metastasis in ccRCC.

Several previous studies revealed that overexpression of Talin-1 is associated with advanced disease and poor prognosis. Lai et al confirmed that increased expression of Talin-1 in OSCC is associated with poor prognosis and knockdown of Talin-1 expression inhibited ability of proliferation and invasion (16). In a recent study by Ji Ling et al. using IHC analysis on colorectal cancer (CRC) and adjacent normal tissue demonstrated that Talin-1 protein expression is upregulated in CRC and knockdown of Talin-1 reduces the proliferation and migration via the epithelial–mesenchymal transition (EMT) signaling pathway (59). Xu N et al. showed that the upregulation of Talin-1 protein in prostate cancer is significantly associated with advanced pathological parameters and predicts lymph node metastases and biochemical recurrence (17). In NPC, authors exhibited that high Talin-1 expression is associated with significantly poorer OS (19). Our present data further is in line with these previous studies and suggest that Talin-1 protein is an important molecule involved in the spread and progression of ccRCC. However, Talin-1 has a different expression in other cancers such as hepatocellular carcinoma (HCC). A previous study by Kanamori et al. (13) showed that high-level expression of Talin-1 in HCC tissues while another study demonstrated that Talin-1 is downregulated in HCC (60), while others showed that expression levels of Talin-1 in serum is significantly higher (61). In addition, Talin was found to be completely absent in endometriosis and endometrioid carcinomas (62). Therefore, it seems that expression levels of Talin-1 are different in various cancers and more investigations are needed to explore the exact mechanism and function of Talin-1 for finding the new ways for therapeutic targeting.

In the present study, for the first time, we showed that membranous, cytoplasmic, and nuclear Talin-1 protein expression in other important subtypes of RCC. We found no significant association between membranous, cytoplasmic, and nuclear

expression of Talin-1 protein and clinicopathological features and patients' outcomes in pRCC cases (type I & II). In chRCCs, a significant association was observed between membranous Talin-1 protein expression and increased tumor stage. Further, we did not find any significant association between expression of Talin-1 protein and survival outcomes. More investigations need to be performed to support these findings using a larger number of cases of each pRCC (type I & II) and chRCC subtypes.

Conclusion

In summary, bioinformatics analysis indicated Talin-1 protein as a potential focal adhesion prognostic marker in RCC. We, therefore, confirmed and validated the expression of Talin-1 protein using the IHC technique in three important subtypes of RCC. Our finding demonstrated that Talin-1 protein is upregulated in human RCC tissues compared to adjacent normal tissues. Our results also for the first time revealed that the statistically significant differences between membranous and cytoplasmic Talin-1 protein expression in various histological subtypes of RCC. A better understanding of the histological subtypes in RCC is urgently needed for further development of treatment options. Moreover, the current study indicates that membranous and cytoplasmic Talin-1 protein expression, particularly cytoplasmic expression compared to nuclear expression plays an important role in more aggressive tumor behaviors, metastasis, and progression of ccRCC. In addition, high membranous and cytoplasmic expression of Talin-1 protein was identified as a worse prognostic variable affecting DSS or PFS in univariate analysis, indicating that Talin-1 may serve as a novel prognostic biomarker in ccRCC if follow up time more extended. However, further studies on the function and mechanism of action of Talin-1 is a requirement to provide new opportunities for therapeutic targeting of RCC.

Abbreviations

RCC: Renal cell carcinoma; ccRCC: clear cell RCC; pRCC: papillary RCC; chRCC: chromophobe RCC; PPI: Protein-protein interaction; FAKs: Focal adhesion kinases; OS: Overall survival; OSCC: Oral squamous cell carcinoma; NPC: Nasopharyngeal carcinoma; FFPE: Formalin-fixed paraffin-embedded; TMAs: Tissue microarrays; IHC: Immunohistochemistry; PRIDE: PRoteomics IDentifications database; GO: Gene ontology; KEGG: Kyoto Encyclopedia of Genes and Genomes; CC: Cellular component; BP: Biological process; MF: Molecular function; CPTAC: Clinical Proteomic Tumor Analysis Consortium; H&E: Hematoxylin and eosin; MVI: Microvascular invasion; LNI: Lymph node invasion; Histological TN: Histological tumor necrosis; DSS: Disease-specific survival; PFS: Progression-free survival; CI: Confidence interval; ECM: Extracellular matrix; FK: Focal adhesion; MMPs: Matrix metalloproteinases; CRC: Colorectal cancer; EMT: Epithelial–mesenchymal transition; HCC: Hepatocellular carcinoma.

Declarations

Ethics Approval and Consent to participate

This study was approved by the Iran University of Medical Sciences Human Research Ethics Committee in Iran (Ref no: IR.IUMS.REC.1398.938). All procedures performed in this study were in accordance with the 1964 Helsinki Declaration and its later amendments. Informed consent was obtained from all individual participants included in the study at the time of sample collection with routine consent forms.

Consent for publication

Informed consent form for publication was obtained from all authors.

Availability of supporting data

All data generated or analyzed during this study are included in this article and the raw data are available from the corresponding author on reasonable request.

Competing interests

The authors declare that they have no competing interests.

Funding

This work was supported by the grant from Iran University of Medical Sciences (Ref no: 16289).

Authors' contributions

LS designed and supervised the work, gathered the paraffin embedded tissues, collected the patient data, prepared the information of patient survival outcomes, analyzed and interpreted the data as well as wrote the manuscript; SV performed the immunohistochemistry examinations and contributed to write the some sections of the manuscript; MA examined hematoxylin and eosin slides, marked the most representative areas in different parts of the tumor for preparing the TMAs blocks, and scored TMAs slides after immunohistochemical staining; FF performed the bioinformatic analysis and wrote the bioinformatic sections in the manuscript. ZM provided for us the laboratory equipment and some materials in this project. All authors read and approved the final manuscript.

Acknowledgements

Not applicable

References

1. Kantarjian H, Koller CA, Wolff RA. The MD Anderson manual of medical oncology: McGraw-hill New York, NY, USA; 2011.
2. Street W. Cancer Facts & Figures 2019. American Cancer Society: Atlanta, GA, USA. 2019.
3. Capitanio U, Bensalah K, Bex A, Boorjian SA, Bray F, Coleman J, et al. Epidemiology of renal cell carcinoma. *European urology*. 2019;75(1):74-84.
4. Siegel Rebecca L, Ahmedin MKDJ. Cancer statistics, 2020.[J]. *CA Cancer J Clin*. 2020;70:7-30.
5. Patil S, Manola J, Elson P, Negrier S, Escudier B, Eisen T, et al. Improvement in overall survival of patients with advanced renal cell carcinoma: prognostic factor trend analysis from an international data set of clinical trials. *The Journal of urology*. 2012;188(6):2095-100.
6. Lalani A-KA, McGregor BA, Albiges L, Choueiri TK, Motzer R, Powles T, et al. Systemic treatment of metastatic clear cell renal cell carcinoma in 2018: current paradigms, use of immunotherapy, and future directions. *European urology*. 2019;75(1):100-10.
7. Duran I, Lambea J, Maroto P, González-Larriba J, Flores L, Granados-Principal S, et al. Resistance to targeted therapies in renal cancer: the importance of changing the mechanism of action. *Targeted oncology*. 2017;12(1):19-35.
8. Motzer RJ, Jonasch E, Agarwal N, Beard C, Bhayani S, Bolger GB, et al. Kidney cancer, version 3.2015. *Journal of the National Comprehensive Cancer Network*. 2015;13(2):151-9.
9. Shruthi BS, Palani Vinodhkumar S. Proteomics: A new perspective for cancer. *Advanced biomedical research*. 2016;5.
10. Pan S, Zhang H, Rush J, Eng J, Zhang N, Patterson D, et al. High throughput proteome screening for biomarker detection. *Molecular & Cellular Proteomics*. 2005;4(2):182-90.
11. Wu X, Al Hasan M, Chen JY. Pathway and network analysis in proteomics. *Journal of theoretical biology*. 2014;362:44-52.
12. Critchley D. Cytoskeletal proteins talin and vinculin in integrin-mediated adhesion. *Biochemical Society Transactions*. 2004;32(5):831-6.
13. Kanamori H, Kawakami T, Effendi K, Yamazaki K, Mori T, Ebinuma H, et al. Identification by differential tissue proteome analysis of talin-1 as a novel molecular marker of progression of hepatocellular carcinoma. *Oncology*. 2011;80(5-6):406-15.

14. Giancotti FG, Ruoslahti E. Integrin signaling. *science*. 1999;285(5430):1028-33.
15. Sakamoto S, McCann RO, Dhir R, Kyprianou N. Talin1 promotes tumor invasion and metastasis via focal adhesion signaling and anoikis resistance. *Cancer research*. 2010;70(5):1885-95.
16. Lai MT, Hua CH, Tsai MH, Wan L, Lin YJ, Chen CM, et al. Talin-1 overexpression defines high risk for aggressive oral squamous cell carcinoma and promotes cancer metastasis. *The Journal of pathology*. 2011;224(3):367-76.
17. Xu N, Chen H-J, Chen S-H, Xue X-Y, Chen H, Zheng Q-S, et al. Upregulation of Talin-1 expression associates with advanced pathological features and predicts lymph node metastases and biochemical recurrence of prostate cancer. *Medicine*. 2016;95(29).
18. Bostanci O, Kemik O, Kemik A, Battal M, Demir U, Purisa S, et al. A novel screening test for colon cancer: Talin-1. *Eur Rev Med Pharmacol Sci*. 2014;18(17):2533-7.
19. Xu Y-F, Ren X-Y, Li Y-Q, He Q-M, Tang X-R, Sun Y, et al. High expression of Talin-1 is associated with poor prognosis in patients with nasopharyngeal carcinoma. *BMC cancer*. 2015;15(1):332.
20. Zanjani LS, Madjd Z, Axcrona U, Abolhasani M, Rasti A, Asgari M, et al. Cytoplasmic expression of B7-H3 and membranous EpCAM expression are associated with higher grade and survival outcomes in patients with clear cell renal cell carcinoma. *Annals of Diagnostic Pathology*. 2020:151483.
21. Vizcaíno JA, Csordas A, Del-Toro N, Dienes JA, Griss J, Lavidas I, et al. 2016 update of the PRIDE database and its related tools. *Nucleic acids research*. 2016;44(D1):D447-D56.
22. Koch E, Finne K, Eikrem Ø, Landolt L, Beisland C, Leh S, et al. Transcriptome-proteome integration of archival human renal cell carcinoma biopsies enables identification of molecular mechanisms. *American Journal of Physiology-Renal Physiology*. 2019;316(5):F1053-F67.
23. Ahmad AA, Paffrath V, Clima R, Busch JF, Rabien A, Kilic E, et al. Papillary Renal Cell Carcinomas Rewire Glutathione Metabolism and Are Deficient in Both Anabolic Glucose Synthesis and Oxidative Phosphorylation. *Cancers*. 2019;11(9):1298.
24. Xiao Y, Clima R, Busch J, Rabien A, Kilic E, Villegas SL, et al. Decreased mitochondrial DNA content drives OXPHOS dysregulation in chromophobe renal cell carcinoma. *Cancer Research*. 2020.
25. Doncheva NT, Morris JH, Gorodkin J, Jensen LJ. Cytoscape StringApp: network analysis and visualization of proteomics data. *Journal of proteome research*. 2018;18(2):623-32.
26. Shannon P, Markiel A, Ozier O, Baliga NS, Wang JT, Ramage D, et al. Cytoscape: a software environment for integrated models of biomolecular interaction networks. *Genome research*. 2003;13(11):2498-504.
27. Pletscher-Frankild S, Pallegà A, Tsafou K, Binder JX, Jensen LJ. DISEASES: Text mining and data integration of disease-gene associations. *Methods*. 2015;74:83-9.
28. Queralt-Rosinach N, Piñero J, Bravo À, Sanz F, Furlong LI. DisGeNET-RDF: harnessing the innovative power of the Semantic Web to explore the genetic basis of diseases. *Bioinformatics*. 2016;32(14):2236-8.
29. Kuleshov MV, Jones MR, Rouillard AD, Fernandez NF, Duan Q, Wang Z, et al. Enrichr: a comprehensive gene set enrichment analysis web server 2016 update. *Nucleic acids research*. 2016;44(W1):W90-W7.
30. Bindea G, Mlecnik B, Hackl H, Charoentong P, Tosolini M, Kirilovsky A, et al. ClueGO: a Cytoscape plug-in to decipher functionally grouped gene ontology and pathway annotation networks. *Bioinformatics*. 2009;25(8):1091-3.
31. Ayob AZ, Ramasamy TS. Cancer stem cells as key drivers of tumour progression. *Journal of biomedical science*. 2018;25(1):1-18.
32. Sidiropoulos K, Viteri G, Sevilla C, Jupe S, Webber M, Orlic-Milacic M, et al. Reactome enhanced pathway visualization. *Bioinformatics*. 2017;33(21):3461-7.
33. Slenter DN, Kutmon M, Hanspers K, Riutta A, Windsor J, Nunes N, et al. WikiPathways: a multifaceted pathway database bridging metabolomics to other omics research. *Nucleic acids research*. 2018;46(D1):D661-D7.

34. Chandrashekar DS, Bashel B, Balasubramanya SAH, Creighton CJ, Ponce-Rodriguez I, Chakravarthi BV, et al. UALCAN: a portal for facilitating tumor subgroup gene expression and survival analyses. *Neoplasia*. 2017;19(8):649-58.
35. Trpkov K, Grignon DJ, Bonsib SM, Amin MB, Billis A, Lopez-Beltran A, et al. Handling and staging of renal cell carcinoma: the International Society of Urological Pathology Consensus (ISUP) conference recommendations. *The American journal of surgical pathology*. 2013;37(10):1505-17.
36. Delahunt B, Cheville JC, Martignoni G, Humphrey PA, Magi-Galluzzi C, McKenney J, et al. The International Society of Urological Pathology (ISUP) grading system for renal cell carcinoma and other prognostic parameters. *The American journal of surgical pathology*. 2013;37(10):1490-504.
37. Moch H, Cubilla AL, Humphrey PA, Reuter VE, Ulbright TM. The 2016 WHO classification of tumours of the urinary system and male genital organs—part A: renal, penile, and testicular tumours. *European urology*. 2016;70(1):93-105.
38. Jourdan F, Sebbagh N, Comperat E, Mourra N, Flahault A, Olschwang S, et al. Tissue microarray technology: validation in colorectal carcinoma and analysis of p53, hMLH1, and hMSH2 immunohistochemical expression. *Virchows Archiv*. 2003;443(2):115-21.
39. Langer R, Von Rahden B, Nahrig J, Von Weyhern C, Reiter R, Feith M, et al. Prognostic significance of expression patterns of c-erbB-2, p53, p16INK4A, p27KIP1, cyclin D1 and epidermal growth factor receptor in oesophageal adenocarcinoma: a tissue microarray study. *Journal of clinical pathology*. 2006;59(6):631-4.
40. Picarda E, Ohaegbulam KC, Zang X. Molecular pathways: targeting B7-H3 (CD276) for human cancer immunotherapy. *Clinical Cancer Research*. 2016;22(14):3425-31.
41. Maziveyi M, Alahari SK. Cell matrix adhesions in cancer: the proteins that form the glue. *Oncotarget*. 2017;8(29):48471.
42. Alizadeh AM, Shiri S, Farsinejad S. Metastasis review: from bench to bedside. *Tumor biology*. 2014;35(9):8483-523.
43. Yoon H, Dehart JP, Murphy JM, Lim S-TS. Understanding the roles of FAK in cancer: inhibitors, genetic models, and new insights. *Journal of Histochemistry & Cytochemistry*. 2015;63(2):114-28.
44. Aye JM, Stafman LL, Williams AP, Garner EF, Stewart JE, Anderson JC, et al. The effects of focal adhesion kinase and platelet-derived growth factor receptor beta inhibition in a patient-derived xenograft model of primary and metastatic Wilms tumor. *Oncotarget*. 2019;10(53):5534.
45. Tai G, Hohenstein P, Davies JA. FAK–Src signalling is important to renal collecting duct morphogenesis: discovery using a hierarchical screening technique. *Biology open*. 2013;2(4):416-23.
46. Béraud C, Dormoy V, Danilin S, Lindner V, Béthry A, Hochane M, et al. Targeting FAK scaffold functions inhibits human renal cell carcinoma growth. *International journal of cancer*. 2015;137(7):1549-59.
47. Murphy JM, Rodriguez YA, Jeong K, Ahn E-YE, Lim S-TS. Targeting focal adhesion kinase in cancer cells and the tumor microenvironment. *Experimental & Molecular Medicine*. 2020:1-10.
48. Zhou J, Yi Q, Tang L. The roles of nuclear focal adhesion kinase (FAK) on Cancer: a focused review. *Journal of Experimental & Clinical Cancer Research*. 2019;38(1):250.
49. M Golubovskaya V. Focal adhesion kinase as a cancer therapy target. *Anti-Cancer Agents in Medicinal Chemistry (Formerly Current Medicinal Chemistry-Anti-Cancer Agents)*. 2010;10(10):735-41.
50. Ljungberg B, Bensalah K, Canfield S, Dabestani S, Hofmann F, Hora M, et al. EAU guidelines on renal cell carcinoma: 2014 update. *European urology*. 2015;67(5):913-24.
51. Lang H, Lindner V, Letourneux H, Martin M, Saussine C, Jacqmin D. Prognostic value of microscopic venous invasion in renal cell carcinoma: long-term follow-up. *European urology*. 2004;46(3):331-5.
52. Bedke J, Heide J, Ribback S, Rausch S, de Martino M, Scharpf M, et al. Microvascular and lymphovascular tumour invasion are associated with poor prognosis and metastatic spread in renal cell carcinoma: a validation study in clinical practice. *Bju International*. 2018;121(1):84-92.
53. Ito K, Seguchi K, Shimazaki H, Takahashi E, Tasaki S, Kuroda K, et al. Tumor necrosis is a strong predictor for recurrence in patients with pathological T1a renal cell carcinoma. *Oncology letters*. 2015;9(1):125-30.

54. Zhang L, Zha Z, Qu W, Zhao H, Yuan J, Feng Y, et al. Tumor necrosis as a prognostic variable for the clinical outcome in patients with renal cell carcinoma: a systematic review and meta-analysis. *BMC cancer*. 2018;18(1):1-13.
55. Laird A, O'Mahony FC, Nanda J, Riddick AC, O'Donnell M, Harrison DJ, et al. Differential expression of prognostic proteomic markers in primary tumour, venous tumour thrombus and metastatic renal cell cancer tissue and correlation with patient outcome. *PloS one*. 2013;8(4):e60483.
56. Thompson RH, Hill JR, Babayev Y, Cronin A, Kaag M, Kundu S, et al. Metastatic renal cell carcinoma risk according to tumor size. *The Journal of urology*. 2009;182(1):41-5.
57. Flem-Karlsen K, Fodstad Ø, Tan M, Nunes-Xavier CE. B7-H3 in cancer—beyond immune regulation. *Trends in Cancer*. 2018;4(6):401-4.
58. Li M, Zhang G, Zhang X, Lv G, Wei X, Yuan H, et al. Overexpression of B7-H3 in CD14+ monocytes is associated with renal cell carcinoma progression. *Medical Oncology*. 2014;31(12):349.
59. Ji L, Jiang F, Cui X, Qin C. Talin1 knockdown prohibits the proliferation and migration of colorectal cancer cells via the EMT signaling pathway. *Oncology letters*. 2019;18(5):5408-16.
60. Zhang J-L, Qian Y-B, Zhu L-X, Xiong Q-R. Talin1, a valuable marker for diagnosis and prognostic assessment of human hepatocellular carcinomas. *Asian Pac J Cancer Prev*. 2011;12(12):3265-9.
61. Youns MM, Abdel Wahab AHA, Hassan ZA, Attia MS. Serum talin-1 is a potential novel biomarker for diagnosis of hepatocellular carcinoma in Egyptian patients. *Asian Pacific journal of cancer prevention*. 2013;14(6):3819-23.
62. Slater M, Cooper M, Murphy C. The cytoskeletal proteins α -actinin, Ezrin, and talin are de-expressed in endometriosis and endometrioid carcinoma compared with normal uterine epithelium. *Applied Immunohistochemistry & Molecular Morphology*. 2007;15(2):170-4.

Tables

Table 1.

Patients and tumor pathological characteristics of histological subtypes of renal cell carcinoma (RCC)

Patients and tumor characteristics	Total samples N (%)	RCC			
		ccRCC N(%)	pRCC N(%)		chRCC N(%)
			Type I	Type II	
Mean age, years (Range)	56 (25-82)	57 (25-82)	57 (33-76)	51 (25-73)	49 (27-76)
≤ Mean age	135 (50.2)	98 (50.3)	11 (55.0)	10 (50.0)	17 (50.0)
> Mean age	134 (49.8)	97 (49.7)	9 (45.0)	10 (50.0)	17 (50.0)
Gender					
Male	183 (68.0)	130 (66.7)	17 (85.0)	16 (80.0)	20 (58.8)
Female	86 (32.0)	65 (33.3)	3 (15.0)	4 (20.0)	14 (41.2)
(Male/Female)	2.1	2.0	5.6	4.0	1.4
Tumor size (cm)					
<4	52 (19.3)	41 (21.0)	4 (20.0)	3 (15.0)	4 (11.8)
4.1–7	97 (36.1)	68 (34.9)	8 (40.0)	6 (30.0)	15 (44.1)
7.1–10	61 (22.7)	49 (25.1)	3 (15.0)	4 (20.0)	5 (14.7)
>10.1	59 (21.9)	37 (19.0)	5 (25.0)	7 (35.0)	10 (29.4)
Nucleolar grade					
I	11 (4.1)	11 (5.6)	0 (0.0)	0 (0.0)	0 (0.0)
II	130 (48.3)	114 (58.5)	13 (65.0)	3 (15.0)	0 (0.0)
III	82 (30.5)	58 (29.7)	7 (35.0)	17 (85.0)	0 (0.0)
IV	12 (4.5)	12 (6.2)	0 (0.0)	0 (0.0)	0 (0.0)
Primary tumor (PT) stage					
pT1	80 (29.7)	66 (33.8)	7 (35.0)	2 (10.0)	5 (14.7)
pT2	27 (10.0)	18 (9.2)	6 (30.0)	1 (5.0)	2 (5.9)
pT3	145 (53.9)	100 (51.3)	7 (35.0)	12 (60.0)	26 (76.5)
pT4	17 (6.3)	11 (5.6)	0 (0.0)	5 (25.0)	1 (2.9)
Microvascular invasion (MVI)					
Present	53 (19.7)	36 (18.5)	2 (10.0)	6 (30.0)	9 (26.5)
Absent	215 (79.9)	159 (81.5)	18 (90.0)	14 (70.0)	24 (70.6)
Not identified	1 (0.4)	0 (0.0)	0 (0.0)	0 (0.0)	1 (2.9)
Lymph node invasion (LNI)					
Involved	14 (5.2)	10 (5.1)	1 (5.0)	3 (15.0)	0 (0.0)
None	208 (77.3)	141 (72.3)	17 (85.0)	16 (80.0)	34 (100.0)
Not identified	47 (17.5)	44 (22.6)	2 (10.0)	1 (5.0)	0 (0.0)
Renal vein invasion					

Present	24 (8.9)	21 (10.8)	0 (0.0)	3 (15.0)	0 (0.0)
Absent	245 (91.1)	174 (89.2)	20 (100.0)	17 (85.0)	34 (100.0)
Histological tumor necrosis (TN)					
Present	109 (40.5)	72 (36.9)	12 (60.0)	15 (75.0)	10 (29.4)
Absent	157 (58.4)	122 (62.6)	8 (40.0)	5 (25.0)	22 (64.7)
Not identified	3 (1.1)	1 (0.5)	0(0.0)	0 (0.0)	2 (5.9)
Renal sinus fat invasion					
Present	149 (55.4)	104 (53.3)	3 (15.0)	17 (85.0)	25 (73.5)
Absent	120 (44.6)	91 (46.7)	17 (85.0)	3 (15.0)	9 (26.5)
Renal pelvis invasion					
Present	30 (11.2)	23 (11.8)	0 (0.0)	7 (35.0)	0 (0.0)
Absent	239 (88.8)	172 (88.2)	20 (100.0)	13 (65.0)	34 (100.0)
Perirenal fat invasion					
Present	59 (21.9)	46 (23.6)	3 (15.0)	4 (20.0)	6 (17.6)
Absent	210 (78.1)	149 (76.4)	17 (85.0)	16 (80.0)	28 (82.4)
Gerota's fascia invasion					
Present	19 (7.1)	19 (9.7)	0 (0.0)	0 (0.0)	0 (0.0)
Absent	250 (92.9)	176 (90.3)	20 (100.0)	20 (100.0)	34 (100.0)
Distant metastasis					
Present	55 (20.4)	46 (23.6)	1 (5.0)	5 (25.0)	3 (8.8)
Absent	214 (79.6)	149 (76.4)	19 (95.0)	15 (75.0)	31 (91.2)
Tumor recurrence					
Yes	41 (15.2)	35 (17.9)	1 (5.0)	2 (10.0)	3 (8.8)
No	228 (84.8)	160 (82.1)	19 (95.0)	18 (90.0)	31 (91.2)
Total	269	195	20	20	34
<i>ccRCC</i> , clear cell renal cell carcinoma, <i>pRCC</i> , papillary renal cell carcinoma, <i>chRCC</i> , chromophobe renal cell carcinoma					

Table 2.

Membranous, cytoplasmic, and nuclear Talin-1 protein expression (Intensity of staining, percentage of positive tumor cells, and H-score) in histological subtypes of RCC

Scoring system	Membranous expression N (%)			Cytoplasmic expression N (%)			Nuclear expression N (%)		
RCC subtypes	ccRCC	pRCC (Type I & II)	chRCC	ccRCC	pRCC (Type I & II)	chRCC	ccRCC	pRCC (Type I & II)	chRCC
Intensity of staining									
No staining (0)	0 (0.0)	0 (0.0)	0 (0.0)	0 (0.0)	0 (0.0)	0 (0.0)	15 (7.7)	17 (42.5)	9 (26.5)
Weak (+1)	22 (11.3)	1 (2.5)	3 (8.8)	29 (14.9)	3 (7.5)	5 (14.7)	70 (35.9)	14 (35.0)	6 (17.6)
Moderate (+2)	74 (37.9)	18 (45.0)	8 (23.5)	70 (35.9)	17 (42.5)	17 (50.0)	74 (37.9)	5 (12.5)	8 (23.5)
Strong (+3)	99 (50.8)	21 (52.5)	23 (67.6)	96 (49.2)	20 (50.0)	12 (35.3)	36 (18.5)	4 (10.0)	11 (32.4)
Percentage of positive tumor cells									
<25%	0 (0.0)	2 (5.0)	0 (0.0)	0 (0.0)	2 (5.0)	0 (0.0)	25 (12.8)	19 (47.5)	12 (35.3)
25–50%	2 (1.0)	2 (5.0)	1 (2.9)	2 (1.0)	2 (5.0)	2 (5.9)	38 (19.5)	5 (12.5)	4 (11.8)
51–75%	19 (9.7)	3 (7.5)	4 (11.8)	25 (12.8)	3 (7.5)	6 (17.6)	23 (11.8)	1 (2.5)	3 (8.8)
>75%	174 (89.2)	33 (82.5)	29 (85.3)	168 (86.2)	33 (82.5)	26 (76.5)	109 (55.9)	15 (37.5)	15 (44.1)
H-score cut off									
Low	99 (50.8)	21 (52.5)	18 (52.9)	102 (52.3)	23 (57.5)	22 (64.7)	99 (50.8)	23 (57.5)	17 (50.0)
High	96 (49.2)	19 (47.5)	16 (47.1)	93 (47.7)	17 (42.5)	12 (35.3)	96 (49.2)	17 (42.5)	17 (50.0)
Total	195	40	34	195	40	34	195	40	34
<i>H-score</i> ; histological score									
<i>RCC</i> ; renal cell carcinoma									
<i>ccRCC</i> ; clear cell renal cell carcinoma, <i>pRCC</i> ; papillary renal cell carcinoma, <i>chRCC</i> ; chromophobe renal cell carcinoma									

Table 3.

Association between median membranous, cytoplasmic, and nuclear Talin-1 protein expression patterns and histological subtypes of RCC

Histological subtypes	Membranous	<i>P-value</i>	Median Q1-Q3	Cytoplasmic	<i>P-value</i>	Median Q1-Q3	Nuclear	<i>P-value</i>	Median Q1-Q3
ccRCC	200	<i>< 0.001</i>	200-300	200	<i>0.003</i>	160-270	100	0.904	50- 200
pRCC	Type I 200		200-300	200		185-300	35		0- 100
	Type II 220		145-300	220		145-300	50.0		0- 100
chRCC	240		200-300	200		120-240	135		0- 210
<p><i>P value</i> is based on Kruskal- Wallis test</p> <p>Values in bold are statistically significant</p> <p><i>RCC</i>; renal cell carcinoma</p> <p><i>ccRCC</i>; clear cell renal cell carcinoma, <i>pRCC</i>; papillary renal cell carcinoma, <i>chRCC</i>; chromophobe renal cell carcinoma</p>									

Table 4.

The association between Talin-1 protein expression and clinicopathological parameters of clear cell renal cell carcinoma (ccRCC)

Patient and tumor characteristics	Total samples N (%)	Membranous expression N (%)		<i>P-value</i>	Cytoplasmic expression N (%)		<i>P-value</i>	Nuclear expression N (%)		<i>P-value</i>
		H-score (cut off = 200) N (%)			H-score (cut off = 200) N (%)			H-score (cut off = 100) N (%)		
		Low (≤ 200)	High (> 200)		Low (≤ 200)	High (> 200)		Low (≤ 100)	High (> 100)	
ccRCC	195 (72.5)	99 (50.8)	96 (49.2)		102 (52.3)	93 (47.7)		99 (50.8)	96 (49.2)	
Mean age, years (Range)	57 (25-82)									
≤ Mean age	98 (50.3)	52 (52.5)	46 (47.9)	0.520	55 (53.9)	43 (46.2)	0.284	52 (52.5)	46 (47.9)	0.520
> Mean age	97 (49.7)	47 (47.5)	50 (52.1)		47 (46.1)	50 (53.8)		47 (47.5)	50 (52.1)	
Gender										
Male	130 (66.7)	67 (67.7)	63 (65.6)	0.761	70 (68.6)	60 (64.5)	0.543	66 (66.7)	64 (66.7)	0.100
Female	65 (33.3)	32 (32.3)	33 (34.4)		32 (31.4)	33 (35.5)		33 (33.3)	32 (33.3)	
Tumor size (cm)										
<4	41 (21.0)	23 (23.2)	18 (18.8)		23 (22.5)	18 (19.4)		18 (18.2)	23 (24.0)	
4.1-7				0.564			0.692			0.523
7.1-10	68 (34.9)	30 (30.3)	38 (39.6)		32 (31.4)	36 (38.7)		34 (34.3)	34 (35.4)	
>10.1	49 (25.1)	27 (27.3)	22 (22.9)		28 (27.5)	21 (22.6)		29 (29.3)	20 (20.8)	
	37 (19.0)	19 (19.2)	18 (18.8)		19 (18.6)	18 (19.4)		18 (18.2)	19 (19.8)	
Nucleolar grade										
I + II	125 (64.1)	77 (77.8)	48 (50.0)	< 0.001	78 (76.5)	47 (50.5)	< 0.001	60 (60.6)	65 (67.7)	
III + IV	70 (35.9)	22 (22.2)	48 (50.0)		24 (23.5)	46 (49.5)		39 (39.4)	31 (32.3)	0.301
Primary tumor (PT) stage										
pT1 + pT2	84 (43.1)	45 (45.5)	39 (40.6)	0.496	45 (44.1)	39 (41.9)	0.759	46 (46.5)	38 (39.6)	0.332
pT3 + pT4	111 (56.9)	54 (54.5)	57 (59.4)		57 (55.9)	54 (58.1)		53 (53.5)	58 (60.4)	
Microvascular invasion (MVI)										
Present	36 (18.5)	11 (11.1)	25 (26.0)	0.007	11 (10.8)	25 (26.9)	0.004	17 (17.2)	19 (19.8)	0.637

Absent	159 (81.5)	88 (88.9)	71 (74.0)		91 (89.2)	68 (73.1)		82 (82.8)	77 (80.2)	
Lymph node invasion (LNI)	10 (5.1)	3 (3.0)	7 (7.3)		3 (2.9)	7 (7.5)		6 (6.1)	4 (4.2)	
Involved	141 (72.3)	76 (76.8)	65 (67.7)	0.250	78 (76.5)	63 (67.7)	0.237	67 (67.7)	74 (77.1)	0.340
None										
Not identified	44 (22.6)	20 (20.2)	24 (25.0)		21 (20.6)	23 (24.7)		26 (26.3)	18 (18.8)	
Renal vein invasion										
Present	21 (10.8)	10 (10.1)	11 (11.5)	0.760	11 (10.8)	10 (10.8)	0.994	11 (11.1)	10 (10.4)	0.876
Absent	174 (89.2)	89 (89.9)	85 (88.5)		91 (89.2)	83 (89.2)		88 (88.9)	86 (89.6)	
Histological tumor necrosis (TN)										
Present	72 (36.9)	28 (28.3)	44 (45.8)		29 (28.4)	43 (46.2)		36 (36.4)	36 (37.5)	
Absent	122 (62.6)	71 (71.7)	51 (53.1)	0.020	73 (71.6)	49 (52.7)	0.018	62 (62.6)	60 (62.5)	0.611
Not identified	1 (0.5)	0 (0.0)	1 (1.0)		0 (0.0)	1 (1.1)		1 (1.0)	0 (0.0)	
Renal sinus fat invasion										
Present	104 (53.3)	48 (48.5)	56 (58.3)	0.168	48 (47.1)	56 (60.2)	0.066	53 (53.5)	51 (53.1)	0.954
Absent	91 (46.7)	51 (51.5)	40 (41.7)		54 (52.9)	37 (39.8)		46 (46.5)	45 (46.9)	
Renal pelvis invasion										
Present	23 (11.8)	7 (7.1)	16 (16.7)	0.038	8 (7.8)	15 (16.1)	0.073	19 (19.2)	4 (4.2)	0.111
Absent	172 (88.2)	92 (92.9)	80 (83.3)		94 (92.5)	78 (83.9)		80 (80.8)	92 (95.8)	
Perirenal fat invasion										
Present	46 (23.6)	19 (19.2)	27 (28.1)	0.142	20 (19.6)	26 (28.0)	0.170	28 (28.3)	18 (18.8)	0.117
Absent	149 (76.4)	80 (80.8)	69 (71.9)		82 (80.4)	67 (72.0)		71 (71.7)	78 (81.3)	
Gerota's fascia invasion										
Present	19 (9.7)	5 (5.1)	14 (14.6)	0.025	6 (5.9)	13 (14.0)	0.050	12 (12.1)	7 (7.3)	0.256
Absent	176 (90.3)	94 (94.9)	82 (85.4)		96 (94.1)	80 (86.0)		87 (87.9)	89 (92.7)	
Distant metastasis										
Present	46 (23.6)	21 (21.2)	25 (26.0)	0.427	23 (22.5)	23 (24.7)	0.720	29 (29.3)	17 (17.7)	0.057
Absent										

	149 (76.4)	78 (78.8)	71 (74.0)		79 (77.5)	70 (75.3)		70 (70.7)	79 (82.3)	
Tumor recurrence										
Yes	35 (17.9)	17 (17.2)	18 (18.8)	0.774	18 (17.6)	17 (18.3)	0.908	20 (20.2)	15 (15.6)	0.405
No	160 (82.1)	82 (82.8)	78 (81.3)		84 (82.4)	76 (81.7)		79 (79.8)	81 (84.4)	
<i>P value</i> , Pearson's chi-square										
<i>H-score</i> , histological score										
Values in bold are statistically significant										

Table 5.

The association between Talin-1 protein expression and clinicopathological parameters of papillary renal cell carcinoma (pRCC) Type I

Patient and tumor characteristics	Total samples N (%)	Membranous expression N (%)		P-value	Cytoplasmic expression N (%)		P-value	Nuclear expression N (%)		P-value
		H-score (cut off = 200) N (%)			H-score (cut off = 200) N (%)			H-score (cut off = 35) N (%)		
		Low (≤ 200)	High (> 200)		Low (≤ 200)	High (> 200)		Low (≤ 35)	High (> 35)	
pRCC Type I	20 (7.45)	11(55.0)	9 (45.0)		13(65.0)	7 (35.0)		10 (50.0)	10 (50.0)	
Mean age, years (Range)	55 (33-76)									
≤ Mean age	11 (55.0)	5 (45.5)	2 (22.2)	0.279	6 (46.2)	1 (14.3)	0.154	4 (40.0)	3 (30.0)	0.639
> Mean age	9 (45.0)	6 (54.5)	7 (77.8)		7 (53.8)	6 (85.7)		6 (60.0)	7 (70.0)	
Gender										
Male	17 (85.0)	9 (81.8)	8 (88.9)	0.660	11 (84.6)	6 (85.7)	0.948	7 (70.0)	10 (100.0)	0.060
Female	3 (15.0)	2 (18.2)	1 (11.1)		2 (15.4)	1 (14.3)		3 (30.0)	0 (0.0)	
Tumor size (cm)										
<4	4 (20.0)	2 (18.2)	2 (22.2)	0.264	3 (23.1)	1 (14.3)	0.086	3 (30.0)	1 (10.0)	0.675
4.1-7	8 (40.0)	6 (54.5)	2 (22.2)		6 (46.2)	2 (28.6)		4 (40.0)	4 (40.0)	
7.1-10	3 (15.0)	2 (18.2)	1 (11.1)		3 (23.1)	0 (0.0)		1 (10.0)	2 (20.0)	
>10.1	5 (25.0)	1 (9.1)	4 (44.4)		1 (7.7)	4 (57.1)		2 (20.0)	3 (30.0)	
Nucleolar grade										
I + II	13 (65.0)	7 (63.6)	6 (66.7)	0.888	8 (61.5)	5 (71.4)	0.658	7 (70.0)	6 (60.0)	0.639
III + IV	7 (35.0)	4 (36.4)	3 (33.3)		5 (38.5)	2 (28.6)		3 (30.0)	4 (40.0)	
Primary tumor (PT) stage										
pT1 + pT2	13 (65.0)	8 (72.7)	5 (55.6)	0.423	9 (69.2)	4 (57.1)	0.589	7 (70.0)	6 (60.0)	0.639
pT3 + pT4	7 (35.0)	3 (27.3)	4 (44.4)		4 (30.8)	3 (42.9)		3 (30.0)	4 (40.0)	
Microvascular invasion (MVI)										
Present	2 (10.0)	1 (9.1)	1 (11.1)	0.881	1 (7.7)	1 (14.3)	0.639	1 (10.0)	1 (10.0)	1.00
Absent	18 (90.0)	10 (90.9)	8 (88.9)		12 (92.3)	6 (85.7)		9 (90.0)	9 (90.0)	

Lymph node invasion (LNI)										
Involved	1 (5.0)	0 (0.0)	1 (11.1)	0.511	0 (0.0)	1 (14.3)	0.231	0 (0.0)	1 (10.0)	0.589
None	17 (85.0)	10 (90.9)	7 (77.8)		11 (84.6)	6 (85.7)		9 (90.0)	8 (80.0)	
Not identified	2 (10.0)	1 (9.1)	1 (11.1)		2 (15.4)	0 (0.0)		1 (10.0)	1 (10.0)	
Renal vein invasion										
Present	0 (0.0)	0 (0.0)	0 (0.0)	*-	0 (0.0)	0 (0.0)	*-	0 (0.0)	0 (0.0)	*-
Absent	20 (100.0)	11 (100.0)	9 (100.0)		13 (100.0)	7 (100.0)		10 (100.0)	10 (100.0)	
Histological tumor necrosis(TN)										
Present	12 (60.0)	6 (54.5)	6 (66.7)	0.582	7 (53.8)	5 (71.4)	0.444	4 (40.0)	8 (80.0)	0.068
Absent	8 (40.0)	5 (45.5)	3 (33.3)		6 (46.2)	2 (28.6)		6 (60.0)	2 (20.0)	
Renal sinus fat invasion										
Present	3 (15.0)	2 (18.2)	1 (11.1)	0.660	2 (15.4)	1 (14.3)	0.948	1 (10.0)	2 (20.0)	0.531
Absent	17 (85.0)	9 (81.8)	8 (88.9)		11 (84.6)	6 (85.7)		9 (90.0)	8 (80.0)	
Renal pelvis invasion										
Present	0 (0.0)	0 (0.0)	0 (0.0)	*-	0 (0.0)	0 (0.0)	*-	0 (0.0)	0 (0.0)	*-
Absent	20 (100.0)	11 (100.0)	9 (100.0)		13 (100.0)	7 (100.0)		10 (100.0)	10 (100.0)	
Perirenal fat invasion										
Present	3 (15.0)	2 (18.2)	1 (11.1)	0.660	3 (23.1)	0 (0.0)	0.168	2 (20.0)	1 (10.0)	0.531
Absent	17 (85.0)	9 (81.8)	8 (88.9)		10 (76.9)	7 (100.0)		8 (80.0)	9 (90.0)	
Gerota's fascia invasion										
Present	0 (0.0)	0 (0.0)	0 (0.0)	*-	0 (0.0)	0 (0.0)	*-	0 (0.0)	0 (0.0)	*-
Absent	20 (100.0)	11 (100.0)	9 (100.0)		13 (100.0)	7 (100.0)		10 (100.0)	10 (100.0)	
Distant metastasis										
Present	1 (5.0)	0 (0.0)	1 (11.1)	0.257	0 (0.0)	1 (14.3)	0.162	0 (0.0)	1 (10.0)	0.305
Absent	19 (95.0)	11 (100.0)	8 (88.9)		13 (100.0)	6 (85.7)		10 (100.0)	9 (90.0)	
Tumor recurrence										
Yes	1 (5.0)	0 (0.0)	1 (11.1)	0.257	0 (0.0)	1 (14.3)	0.162	0 (0.0)	1 (10.0)	0.305
No	19 (95.0)	11 (100.0)			13 (100.0)			10 (100.0)		

	8 (88.9)	6 (85.7)	9 (90.0)
<i>P value</i> ; Pearson's chi-square			
<i>H-score</i> ; histological score			
*: No statistical are computed because the parameter is constant			

Table 6.

The association between Talin-1 protein expression and clinicopathological parameters of papillary renal cell carcinoma (pRCC) Type II

Patient and tumor characteristics	Total samples N (%)	Membranous expression N (%)		P-value	Cytoplasmic expression N (%)		P-value	Nuclear expression N (%)		P-value
		H-score (cut off = 220) N (%)			H-score (cut off = 220) N (%)			H-score (cut off = 50) N (%)		
		Low (≤ 220)	High (> 220)		Low (≤ 220)	High (> 220)		Low (≤ 50)	High (> 50)	
pRCC Type II	20 (7.45)	10 (50.0)	10 (50.0)		10 (50.0)	10 (50.0)		11 (55.0)	9 (45.0)	
Mean age, years (Range)	53 (25-73)									
≤ Mean age	10 (50.0)	7 (70.0)	3 (30.0)	0.074	7 (70.0)	3 (30.0)	0.074	6 (54.5)	4 (44.4)	0.653
> Mean age	10 (50.0)	3 (30.0)	7 (70.0)		3 (30.0)	7 (70.0)		5 (45.5)	5 (55.6)	
Gender										
Male	16 (80.0)	8 (80.0)	8 (80.0)	1.000	8 (80.0)	8 (80.0)	1.000	9 (81.8)	7 (77.8)	0.822
Female	4 (20.0)	2 (20.0)	2 (20.0)		2 (20.0)	2 (20.0)		2 (18.2)	2 (22.2)	
Tumor size (cm)										
<4	3 (15.0)	3 (30.0)	0 (0.0)	0.246	3 (30.0)	0 (0.0)	0.246	1 (9.1)	2 (22.2)	0.698
4.1-7	6 (30.0)	3 (30.0)	3 (30.0)		3 (30.0)	3 (30.0)		3 (27.3)	3 (33.3)	
7.1-10	4 (20.0)	3 (30.0)	3 (30.0)		1 (10.0)	3 (30.0)		2 (18.2)	2 (22.2)	
>10.1	7 (35.0)	1 (10.0)	4 (40.0)		3 (30.0)	4 (40.0)		5 (45.5)	2 (22.2)	
Nucleolar grade										
I + II	3 (15.0)	2 (20.0)	1 (10.0)	0.531	2 (20.0)	1 (10.0)	0.531	2 (18.2)	1 (11.1)	0.660
III + IV	17 (85.0)	8 (80.0)	9 (90.0)		8 (80.0)	9 (90.0)		9 (81.8)	8 (88.9)	
Primary tumor (PT) stage										
pT1 + pT2	3 (15.0)	1 (10.0)	2 (20.0)	0.531	1 (10.0)	2 (20.0)	0.531	0 (0.0)	3 (33.3)	0.058
pT3 + pT4	17 (85.0)	9 (90.0)	8 (80.0)		9 (90.0)	8 (80.0)		11 (100.0)	6 (66.7)	
Microvascular invasion (MVI)										
Present	6 (30.0)	4 (40.0)	2 (20.0)	0.329	4 (40.0)	2 (20.0)	0.329	4 (36.4)	2 (22.2)	0.492
Absent	14 (70.0)									

		6 (60.0)	8 (80.0)		6 (60.0)	8 (80.0)		7 (63.6)	7 (77.8)	
Lymph node invasion (LNI)										
Involved	3 (15.0)	3 (30.0)	0 (0.0)		3 (30.0)	0 (0.0)		2 (18.2)	1 (11.1)	
None	16 (80.9)	6 (60.0)	10 (100.0)	0.082	6 (60.0)	10 (100.0)	0.082	8 (72.7)	8 (88.9)	0.564
Not identified	1 (5.0)	1 (10.0)	0 (0.0)		1 (10.0)	0 (0.0)		1 (9.1)	0 (0.0)	
Renal vein invasion										
Present	3 (15.0)	3 (30.0)	0 (0.0)	0.060	3 (30.0)	0 (0.0)	0.060	2 (18.2)	1 (11.1)	0.660
Absent	17 (85.0)	7 (70.0)	10 (100.0)		7 (70.0)	10 (100.0)		9 (81.8)	8 (88.9)	
Histological tumor necrosis(TN)										
Present	15 (75.0)	6 (60.0)	9 (90.0)	0.121	6 (60.0)	9 (90.0)	0.121	8 (72.7)	7 (77.8)	0.795
Absent	5 (25.0)	4 (40.0)	1 (10.0)		4 (40.0)	1 (10.0)		3 (27.3)	2 (22.2)	
Renal sinus fat invasion										
Present	17 (85.0)	8 (80.0)	9 (90.0)	0.531	8 (80.0)	9 (90.0)	0.531	10 (90.9)	7 (77.8)	0.413
Absent	3 (15.0)	2 (20.0)	1 (10.0)		2 (20.0)	1 (10.0)		1 (9.1)	2 (22.2)	
Renal pelvis invasion										
Present	7 (35.0)	5 (50.0)	2 (20.0)	0.160	5 (50.0)	2 (20.0)	0.160	4 (36.4)	3 (33.3)	0.888
Absent	13 (65.0)	5 (50.0)	8 (80.0)		5 (50.0)	8 (80.0)		7 (63.6)	6 (66.7)	
Perirenal fat invasion										
Present	4 (20.0)	3 (30.0)	1 (10.0)	0.264	3 (30.0)	1 (10.0)	0.264	3 (27.3)	1 (11.1)	0.369
Absent	16 (80.0)	7 (70.0)	9 (90.0)		7 (70.0)	9 (90.0)		8 (72.7)	8 (88.9)	
Gerota's fascia invasion										
Present	0 (0.0)	0 (0.0)	0 (0.0)	*-	0 (0.0)	0 (0.0)	*-	0 (0.0)	0 (0.0)	*-
Absent	20 (100.0)	10 (100.0)	10 (100.0)		10 (100.0)	10 (100.0)		11 (100.0)	9 (100.0)	
Distant metastasis										
Present	5 (25.0)	3 (30.0)	2 (20.0)	0.606	3 (30.0)	2 (20.0)	0.606	4 (36.4)	1 (11.1)	0.194
Absent	15 (75.0)	7 (70.0)	8 (80.0)		7 (70.0)	8 (80.0)		7 (63.6)	8 (88.9)	
Tumor recurrence										

Yes	2 (10.0)	1 (10.0)	1 (10.0)	1.000	1 (10.0)	1 (10.0)	1.000	2 (18.2)	0 (0.0)	0.178
No	18 (90.0)	9 (90.0)	9 (90.0)		9 (90.0)	9 (90.0)		9 (81.8)	9 (100.0)	
<i>P value</i> , Pearson's chi-square										
<i>H-score</i> , histological score										
*: No statistical are computed because the parameter is constant										

Table 7.

The association between Talin-1 protein expression and clinicopathological parameters of chromophobe renal cell carcinoma (chRCC)

Patient and tumor characteristics	Total samples N (%)	Membranous expression N (%)		P-value	Cytoplasmic expression N (%)		P-value	Nuclear expression N (%)		P-value
		H-score (cut off = 240) N (%)			H-score (cut off = 200) N (%)			H-score (cut off = 135) N (%)		
		Low (≤ 240)	High (> 240)		Low (≤ 200)	High (> 200)		Low (≤ 135)	High (> 135)	
chRCC	34 (12.6)	18 (52.9)	16 (47.1)		22 (64.7)	12 (35.3)		17 (50.0)	17 (50.0)	
Mean age, years (Range)	49 (27-76)									
≤ Mean age	17 (50.0)	8 (44.4)	9 (56.3)	0.492	9 (40.9)	8 (66.7)	0.151	7 (41.2)	10 (58.8)	0.303
> Mean age	17 (50.0)	10 (55.6)	7 (43.8)		13 (59.1)	4 (33.3)		10 (58.8)	7 (41.2)	
Gender										
Male	20 (58.8)	10 (55.6)	10 (62.5)	0.681	12 (54.5)	8 (66.7)	0.493	10 (58.8)	10 (58.8)	0.100
Female	14 (41.2)	8 (44.4)	6 (37.5)		10 (45.5)	4 (33.3)		7 (41.2)	7 (41.2)	
Tumor size (cm)										
<4	4 (11.8)	3 (16.7)	1 (6.3)		3 (13.6)	1 (8.3)		1 (5.9)	3 (17.6)	
4.1-7	15 (44.1)	9 (50.0)	6 (37.5)	0.554	9 (40.9)	6 (50.0)	0.918	10 (58.8)	5 (29.4)	0.352
7.1-10	5 (14.7)	2 (11.1)	3 (18.8)		3 (13.6)	2 (16.7)		2 (11.8)	3 (17.6)	
>10.1	10 (29.4)	4 (22.2)	6 (37.5)		7 (31.8)	3 (25.0)		4 (23.5)	6 (35.3)	
Primary tumor (PT) stage										
pT1 + pT2	7 (20.6)	6 (33.3)	1 (6.3)	0.050	4 (18.2)	3 (25.0)	0.639	5 (29.4)	2 (11.8)	0.203
pT3 + pT4	27 (79.4)	12 (66.7)	15 (93.8)		18 (81.8)	9 (75.0)		12 (70.6)	15 (88.2)	
Microvascular invasion (MVI)										
Present	9 (26.5)	2 (11.1)	7 (43.8)		6 (27.3)	3 (25.0)		5 (29.4)	4 (23.5)	
Absent	24 (70.6)	15 (83.3)	9 (56.3)	0.075	16 (72.7)	8 (66.7)	0.389	12 (70.6)	12 (70.6)	0.574
Not identified	1 (2.9)	1 (5.6)	0 (0.0)		0 (0.0)	1 (8.3)		0 (0.0)	1 (5.9)	
Lymph node invasion (LNI)										
Involved	0 (0.0)	0 (0.0)	0 (0.0)	*-	0 (0.0)	0 (0.0)	*-	0 (0.0)	0 (0.0)	*-

None	34 (100.0)	18 (100.0)	16 (100.0)		22 (100.0)	12 (100.0)		17 (100.0)	17 (100.0)	
Renal vein invasion	0 (0.0)	0 (0.0)	0 (0.0)	*-	0 (0.0)	0 (0.0)	*-	0 (0.0)	0 (0.0)	*-
Present										
Absent	34 (100.0)	18 (100.0)	16 (100.0)		22 (100.0)	12 (100.0)		17 (100.0)	17 (100.0)	
Histological tumor necrosis(TN)										
Present	10 (29.4)	5 (27.8)	5 (31.3)	0.389	7 (31.8)	3 (25.0)	0.851	6 (35.3)	4 (23.5)	0.748
Absent	22 (64.7)	11 (61.1)	11 (68.8)		14 (63.6)	8 (66.7)		10 (58.8)	12 (70.6)	
Not identified	2 (5.9)	2 (11.1)	0 (0.0)		1 (4.5)	1 (8.3)		1 (5.9)	1 (5.9)	
Renal sinus fat invasion										
Present	25 (73.5)	13 (72.2)	12 (75.0)	0.855	17 (77.3)	8 (66.7)	0.503	13 (76.5)	12 (70.6)	0.697
Absent	9 (26.5)	5 (27.8)	4 (25.0)		5 (22.7)	4 (33.3)		4 (23.5)	5 (29.4)	
Renal pelvis invasion										
Present	0 (0.0)	0 (0.0)	0 (0.0)	*-	0 (0.0)	0 (0.0)	*-	0 (0.0)	0 (0.0)	*-
Absent	34 (100.0)	18 (100.0)	16 (100.0)		22 (100.0)	12 (100.0)		17 (100.0)	17 (100.0)	
Perirenal fat invasion										
Present	6 (17.6)	2 (11.1)	4 (25.0)	0.289	6 (27.3)	0 (0.0)	0.056	3 (17.6)	3 (17.6)	1.000
Absent	28 (82.4)	16 (88.9)	12 (75.0)		16 (72.7)	12 (100.0)		14 (82.4)	14 (82.4)	
Gerota's fascia invasion										
Present	0 (0.0)	0 (0.0)	0 (0.0)	*-	0 (0.0)	0 (0.0)	*-	0 (0.0)	0 (0.0)	*-
Absent	34 (100.0)	18 (100.0)	16 (100.0)		22 (100.0)	12 (100.0)		17 (100.0)	17 (100.0)	
Distant metastasis										
Present	3 (8.8)	2 (11.1)	1 (6.3)	0.618	3 (13.6)	0 (0.0)	0.180	3 (17.6)	0 (0.0)	0.070
Absent	31 (91.2)	16 (88.9)	15 (93.8)		19 (86.4)	12 (100.0)		14 (82.4)	17 (100.0)	
Tumor recurrence										
Yes	3 (8.8)	3 (16.7)	0 (0.0)	0.087	2 (9.1)	1 (8.3)	0.941	2 (11.8)	1 (5.9)	0.545
No	31 (91.2)	15 (83.3)	16 (100.0)		20 (90.9)	11 (91.7)		15 (88.2)	16 (94.1)	
<i>P value</i> ; Pearson's chi-square										
<i>H-score</i> ; histological score										

Values in bold are statistically significant

* : No statistical are computed because the parameter is constant

Table 8.

The main characteristics of patients enrolled for survival analysis according to histological subtypes of RCC

Features	Histological subtypes of RCC			
	ccRCC N (%)	pRCC N (%)		chRCC N (%)
		Type I	Type II	
Number of patients (N)	195	20	20	34
Follow-up period (month)	117	80	77	77
Mean duration of follow-up time (month) (SD)	53 (30.2)	54 (19.9)	46 (21.3)	48 (15.3)
Median duration of follow-up time (month) (Q1, Q3)	51 (31, 74)	53 (41, 76)	41 (28, 66)	47 (36, 61)
Cancer-related death (N %)	34 (17.4)	1 (5.0)	3 (15.0)	2 (5.9)
Distant metastasis during follow-up (N %)	48 (24.6)	1 (5.0)	5 (25.0)	3 (8.8)
Tumor recurrence during follow-up (N %)	37 (19.0)	1 (5.0)	2 (10.0)	3 (8.8)
Alive patients without distant metastasis and tumor recurrence (N %)	140 (71.8)	19 (95.0)	15 (75.0)	30 (88.2)
<i>RCC</i> ; renal cell carcinoma				
<i>ccRCC</i> ; clear cell renal cell carcinoma, <i>pRCC</i> ; papillary renal cell carcinoma, <i>chRCC</i> ; chromophobe renal cell carcinoma				

Table 9.

Univariate and multivariate cox regression analyses of potential prognostic factors for disease-specific survival (DSS) in patients with clear cell RCC (ccRCC)

Covariate	Univariate analysis		Multivariate analysis (Membranous)		Multivariate analysis (Cytoplasmic)	
	HR (95% CI)	P-value	HR (95% CI)	P-value	HR (95% CI)	P-value
Membranous Talin-1 expression						
High versus low	2.024 (1.007-4.067)	0.048	1.434 (0.667-3.084)	0.356	-	-
Cytoplasmic Talin-1 expression						
High versus low	2.188 (1.089-4.398)	0.028	-	-	1.601 (0.756-3.394)	0.219
Nuclear Talin-1 expression						
High versus low	0.615 (0.310-1.222)	0.165	-	-	-	-
Tumor size (cm)		0.009		0.354		0.359
4.1- 7 versus <4	1.656 (0.439-6.241)	0.457	1.203 (0.309-4.683)	0.790	1.216 (0.313-4.726)	0.778
7.1-10 versus <4		0.043		0.263		0.256
10.1 versus <4	3.694 (1.042-13.095)	0.007	2.225 (0.549-9.018)	0.180	2.254 (0.554-9.165)	0.181
	5.632 (1.588-19.974)		2.688 (0.634-11.400)		2.684 (0.632-11.392)	
Nucleolar grade						
III + IV versus I + II	4.144 (2.059-8.339)	<0.001	2.563 (1.119-5.869)	0.026	2.483 (1.095-5.633)	0.029
Primary tumor (PT) stage						
pT3 + pT4 versus pT1 + pT2	2.266 (1.085-4.732)	0.029	1.223 (0.533-2.805)	0.635	1.237 (0.538-2.842)	0.617
Microvascular invasion (MVI)	0.292 (0.148-0.575)	<0.001	-	-	-	-
Renal vein invasion	0.349 (0.159-0.770)	0.009	-	-	-	-
Histological tumor necrosis (TN)	0.397 (0.203-0.773)	0.007	-	-	-	-
Renal pelvis invasion	0.0422 (0.191-0.932)	0.033	-	-	-	-
Perirenal fat invasion	0.265 (0.137-0.515)	<0.001	-	-	-	-
Gerota's fascia invasion	0.341 (0.153-0.758)	0.008	-	-	-	-
Distant metastasis	0.012 (0.003-0.052)	<0.001	-	-	-	-
Tumor recurrence	0.060 (0.029-	<0.001	-	-	-	-

HR; hazard ratio, CI, confidence interval

The variables with *P* value less than 0.05 and HR more than 1.0 were included in multivariable analyses

Values in bold are statistically significant

Table 10.

Univariate and multivariate cox regression analyses of potential prognostic factors for progression-free survival (PFS) in patients with clear cell RCC (ccRCC)

Covariate	Univariate analysis		Multivariate analysis (Cytoplasmic)	
	HR (95% CI)	<i>P</i> -value	HR (95% CI)	<i>P</i> -value
Membranous Talin-1 expression				
High versus low	1.748 (0.922- 3.316)	0.087	-	-
Cytoplasmic Talin-1 expression				
High versus low	1.889 (1.000- 3.584)	0.050	1.430 (0.715- 2.863)	0.312
Nuclear Talin-1 expression				
High versus low	0.675 (0.359- 1.272)	0.225	-	-
Tumor size (cm)		0.004		0.142
4.1- 7 versus <4	1.892 (0.512- 6.990)	0.339	1.543 (0.408- 5.840)	0.523
7.1-10 versus <4	4.327 (1.243- 15.063)	0.021	3.152 (0.818- 12.141)	0.095
10.1 versus <4	6.315 (1.814- 21.987)	0.004	3.702 (0.921- 14.878)	0.065
Nucleolar grade				
III + IV versus I + II	3.666 (1.929- 6.968)	<0.001	2.243 (1.061- 4.739)	0.034
Primary tumor (PT) stage				
pT3 + pT4 versus pT1 + pT2	1.986 (1.008- 3.913)	0.047	1.044 (0.492- 2.217)	0.910
Microvascular invasion (MVI)	0.310 (0.163- 0.588)	<0.001	-	-
Renal vein invasion	0.350 (0.166- 0.737)	0.006	-	-
Histological tumor necrosis (TN)	0.445 (0.239- 0.827)	0.010	-	-
Perirenal fat invasion	0.239 (0.128- 0.444)	<0.001	-	-
Gerota's fascia invasion	0.396 (0.181- 0.864)	0.020	-	-
Distant metastasis	0.032 (0.014- 0.074)	<0.001	-	-
Tumor recurrence	0.080 (0.041- 0.155)	<0.001	-	-
HR; hazard ratio, CI, confidence interval The variables with <i>P</i> value less than 0.05 and HR more than 1.0 were included in multivariable analyses Values in bold are statistically significant				

Table 11.

The association between cytoplasmic Talin-1/B7H3 phenotypes and clinicopathological parameters of clear cell renal cell carcinoma (ccRCC)

Patient and tumor characteristics	Total samples N (%)	Talin-1/B7H3 phenotypes				<i>P-value</i>
		Talin-1 High /	Talin-1 High /	Talin-1 Low /	Talin-1 Low /	
		B7H3 ^{High}	B7H3 ^{Low}	B7H3 ^{High}	B7H3 ^{Low}	
ccRCC	138 (100.0)	41 (29.7)	21 (15.2)	26 (18.8)	50 (36.2)	
Mean age, years (Range)	57 (25-82)					
≤ Mean age	65 (47.1)	18 (43.9)	10 (47.6)	16 (61.5)	21 (42.0)	0.412
> Mean age	73 (52.9)	23 (56.1)	11 (52.4)	10 (38.5)	29 (58.0)	
Gender						
Male	91 (65.9)	27 (65.9)	11 (52.4)	18 (69.2)	35 (70.0)	0.530
Female	47 (34.1)	14 (34.1)	10 (47.6)	8 (30.8)	15 (30.0)	
Tumor size (cm)						
<4	29 (21.0)	7 (17.1)	5 (23.8)	6 (23.1)	11 (22.0)	0.599
4.1-7	49 (35.5)	13 (31.7)	10 (47.6)	6 (23.1)	20 (40.0)	
7.1-10	32 (23.2)	10 (24.4)	5 (23.8)	7 (26.9)	10 (20.0)	
>10.1	28 (20.3)	11 (26.8)	1 (4.8)	7 (26.9)	9 (18.0)	
Nucleolar grade						
I + II	86 (62.3)	18 (43.9)	13 (61.9)	14 (53.8)	41 (82.0)	0.002
III + IV	52 (37.7)	23 (56.1)	8 (38.1)	12 (46.2)	9 (18.0)	
Primary tumor (PT) stage						
pT1 + pT2	54 (39.1)	14 (34.1)	11 (52.4)	12 (46.2)	17 (34.0)	0.381
pT3 + pT4	84 (60.9)	27 (65.9)	10 (47.6)	14 (53.8)	33 (66.0)	
Microvascular invasion (MVI)						
Present	29 (21.0)	16 (39.0)	2 (9.5)	7 (26.9)	4 (8.0)	0.002
Absent	109 (79.0)	25 (61.0)	19 (90.5)	19 (73.1)	46 (92.0)	
Lymph node invasion (LNI)						
Involved	7 (5.1)	5 (12.2)	1 (4.8)	0 (0.0)	1 (2.0)	0.177
None	108 (78.3)	28 (68.3)	18 (85.7)	20 (76.9)	42 (84.0)	
Not identified	23 (16.7)	8 (19.5)	2 (9.5)	6 (23.1)	7 (14.0)	
Renal vein invasion						
Present	13 (9.4)	3 (7.3)	0 (0.0)	5 (19.2)	5 (10.0)	0.148
Absent	125 (90.6)	38 (92.7)	21 (100.0)	21 (80.8)	45 (90.0)	
Histological tumor necrosis (TN)						
Present						

Absent	48 (34.8)	22 (53.7)	3 (14.3)	9 (34.6)	14 (28.0)	0.026
Not identified	89 (64.5)	18 (43.9)	18 (85.7)	17 (65.4)	36 (72.0)	
	1 (0.7)	1 (2.4)	0 (0.0)	0 (0.0)	0 (0.0)	
Renal sinus fat invasion						
Present	77 (55.8)	27 (65.9)	11 (52.4)	13 (50.0)	26 (52.0)	0.489
Absent	61 (44.2)	14 (34.1)	10 (47.6)	13 (50.0)	24 (48.0)	
Renal pelvis invasion						
Present	10 (7.2)	4 (9.8)	1 (4.8)	1 (3.8)	4 (8.0)	0.785
Absent	128 (92.8)	37 (90.2)	20 (95.2)	25 (96.2)	46 (92.0)	
Perirenal fat invasion						
Present	28 (20.3)	10 (24.4)	1 (4.8)	7 (26.9)	10 (20.0)	0.234
Absent	110 (79.7)	31 (75.6)	20 (95.2)	19 (73.1)	40 (80.0)	
Gerota's fascia invasion						
Present	10 (7.2)	5 (12.2)	1 (4.8)	4 (15.4)	0 (0.0)	0.043
Absent	128 (92.8)	36 (87.8)	20 (95.2)	22 (84.6)	50 (100.0)	
Distant metastasis						
Present	36 (26.1)	14 (34.1)	2 (9.5)	11 (42.3)	9 (18.0)	0.022
Absent	102 (73.9)	27 (65.9)	19 (90.5)	15 (57.7)	41 (82.0)	
Tumor recurrence						
Yes	29 (21.0)	10 (24.4)	4 (19.0)	7 (26.9)	8 (16.0)	0.652
No	109 (79.0)	31 (75.6)	17 (81.0)	19 (73.1)	42 (84.0)	
<i>P value</i> ; Pearson's chi-square						
Values in bold are statistically significant						

Figures

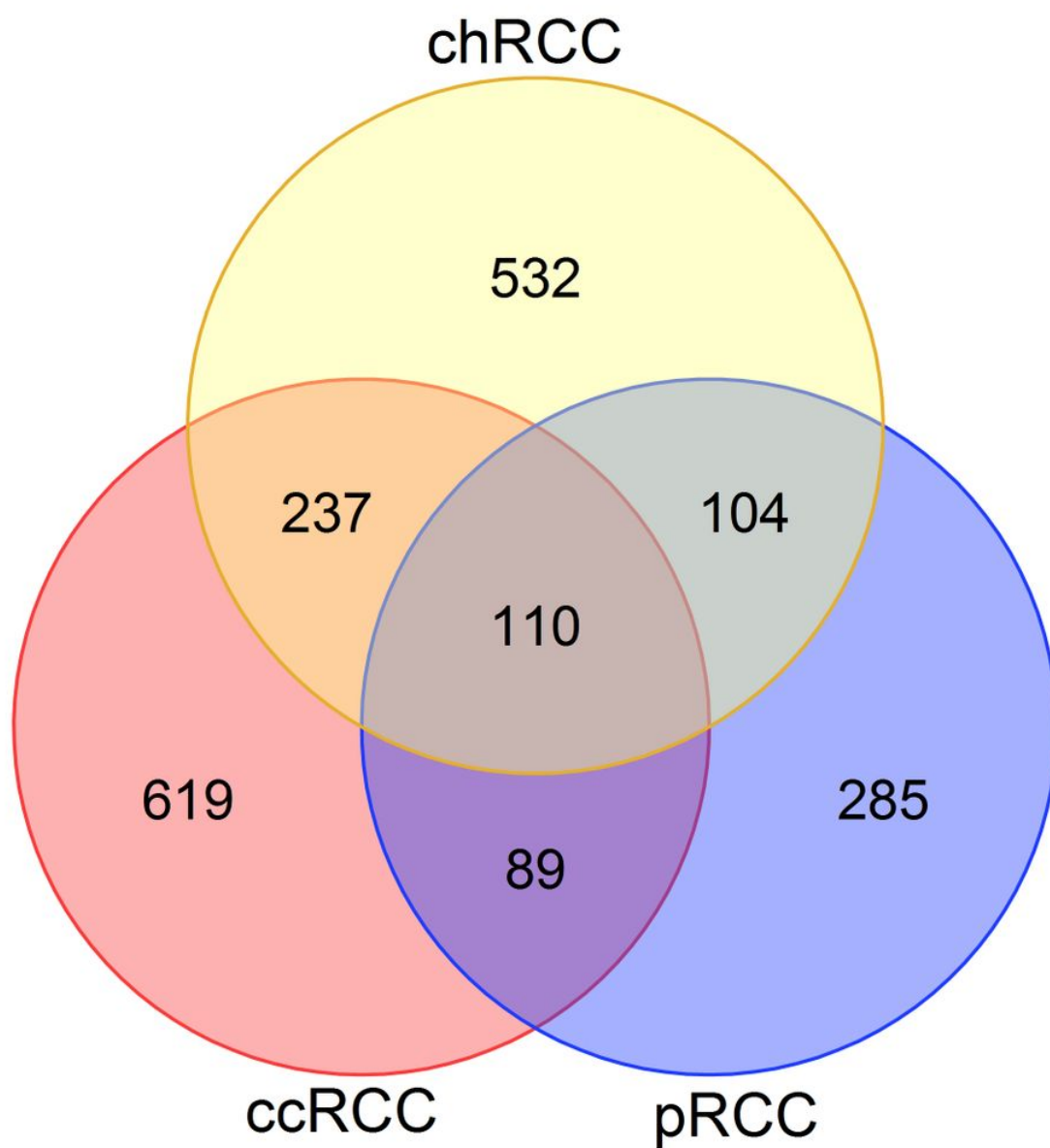


Figure 1

Venn diagram represents the overlaps of differential protein expressions between three subtypes of renal cell carcinoma (RCC). One hundred and ten common differential protein expressions obtained based on proteomics data from previous articles, including PMID: 30838877, PMID: 31484429, and PMID: 32694149 for clear cell RCC (ccRCC), papillary RCC (pRCC), and chromophobe RCC (chRCC), respectively.

Figure 3

Pathway analysis and crosslink figure of pathways using ClueGO for hub genes related to cancer. Pathway analysis indicated that several genes such as TLN1 (Talin-1) were interconnected to focal adhesion (KA) and extracellular matrix (ECM) pathways. The genes collected together in close pathways.

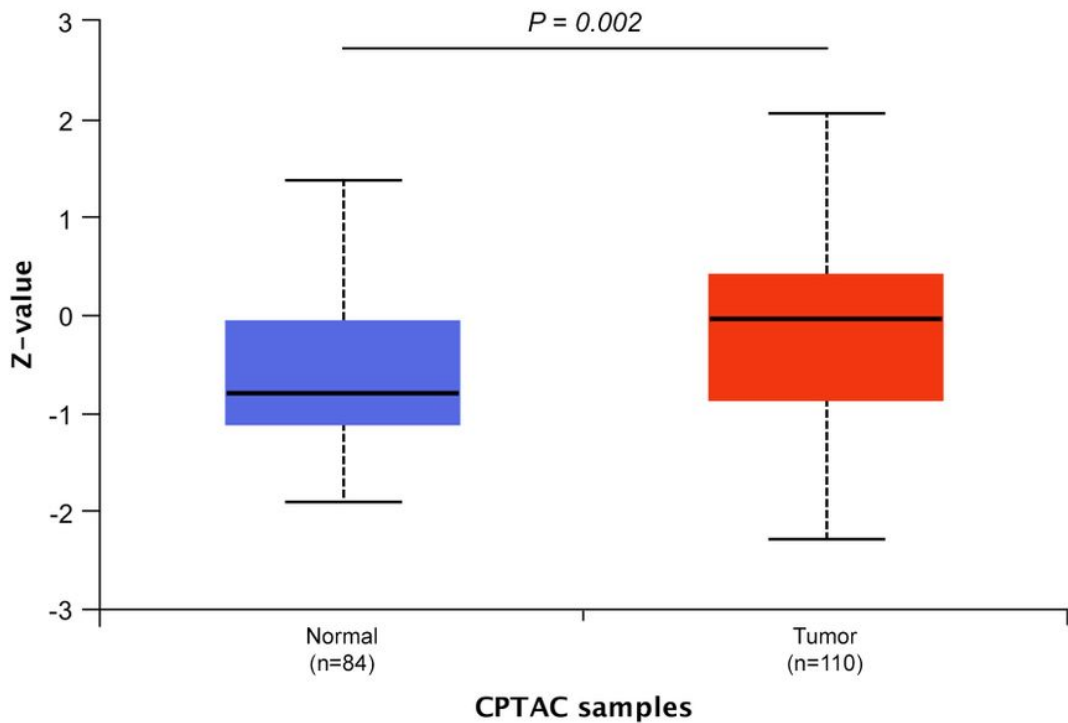


Figure 4

Box plot results of clinical proteomic tumor analysis consortium (CPTAC) for Talin-1 protein expression on UALCAN database. The results showed an increased expression of Talin-1 protein in ccRCCs compared to normal tissue samples with a statistically significant association ($P= 0.002$). Z-value represents standard deviations from the median across samples for the given cancer type.

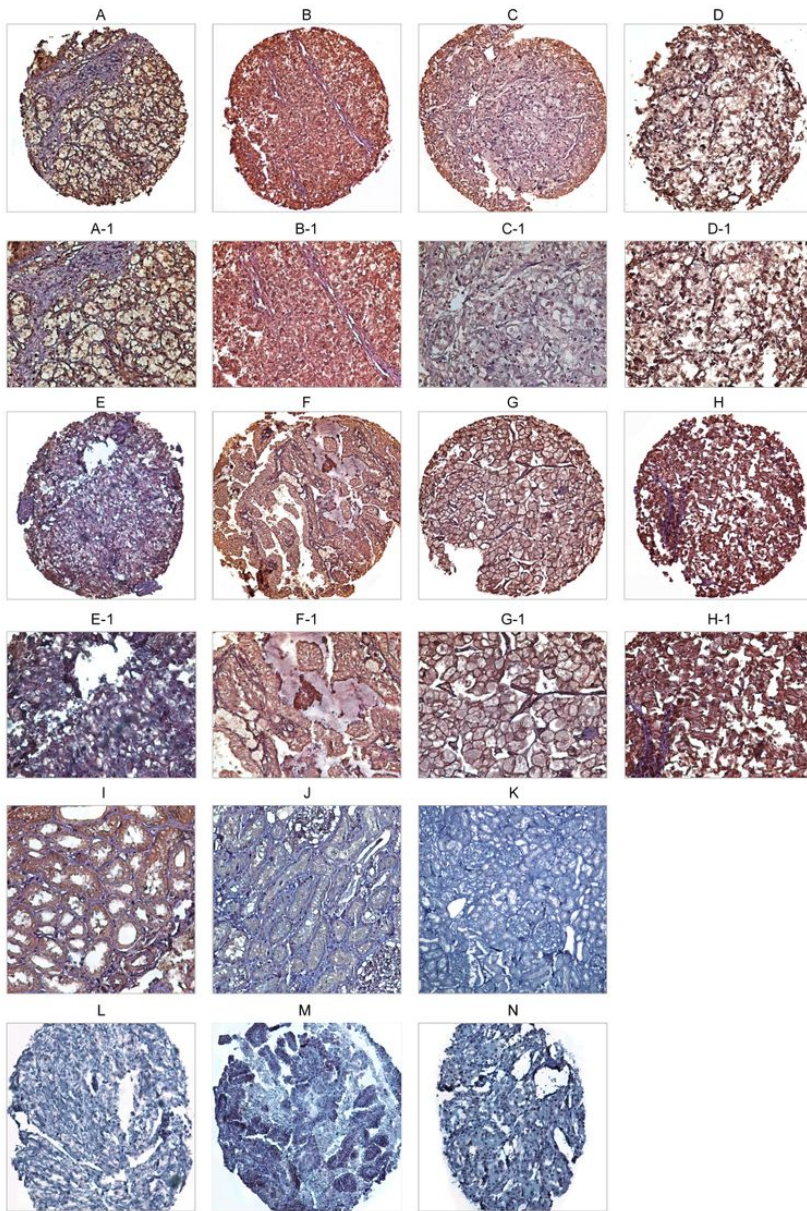


Figure 5

Immunohistochemical analysis of Talin-1 protein expression in three subtypes of renal cell carcinoma (RCC) tissues. Talin-1 protein expression in clear cell renal cell carcinoma (ccRCC): low membranous and cytoplasmic expression (A, A-1), high membranous and cytoplasmic expression (B, B-1), low nuclear expression (C, C-1), and high nuclear expression (D, D-1). Talin-1 protein expression in papillary RCC (pRCC): low expression (E, E-1) and high expression (F, F-1). In chromophobe RCC (chRCC): low expression (G, G-1) and high expression (H, H-1). IHC staining of adjacent normal tissue (I), and human normal kidney as (J) positive and (K) negative controls. Isotype controls in immunohistochemistry staining in ccRCC (L), pRCC (M), and chRCC (N). Figures are shown with lowercase letters have a magnification of 100 × and those with uppercase letters have a magnification of 200×.

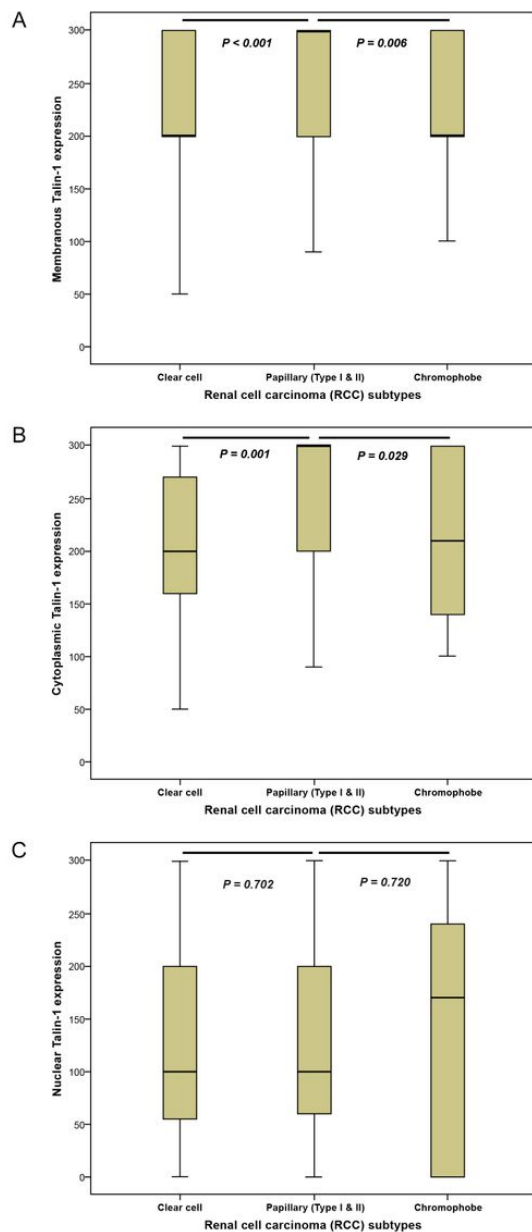


Figure 6

The median membranous, cytoplasmic, and nuclear expression levels of Talin-1 protein in various subtypes of renal cell carcinoma (RCC) including clear cell, papillary (type I and II), and chromophobe RCC using Mann–Whitney U test. (A) The results showed there is a statistically significant difference in membranous Talin-1 protein expression between ccRCC and pRCC ($P < 0.001$) and between pRCC and chRCC ($P = 0.006$). (B) A significant difference was found in cytoplasmic Talin-1 protein expression between ccRCC and pRCC cases ($P = 0.001$) and between pRCC and chRCC ($P = 0.029$). (C) There was no statistically significant difference in the median expression level of nuclear Talin-1 protein between the subtypes of RCC. On the basis of the standard definitions, each box-plot shows the median (bold line) and interquartile line (box).

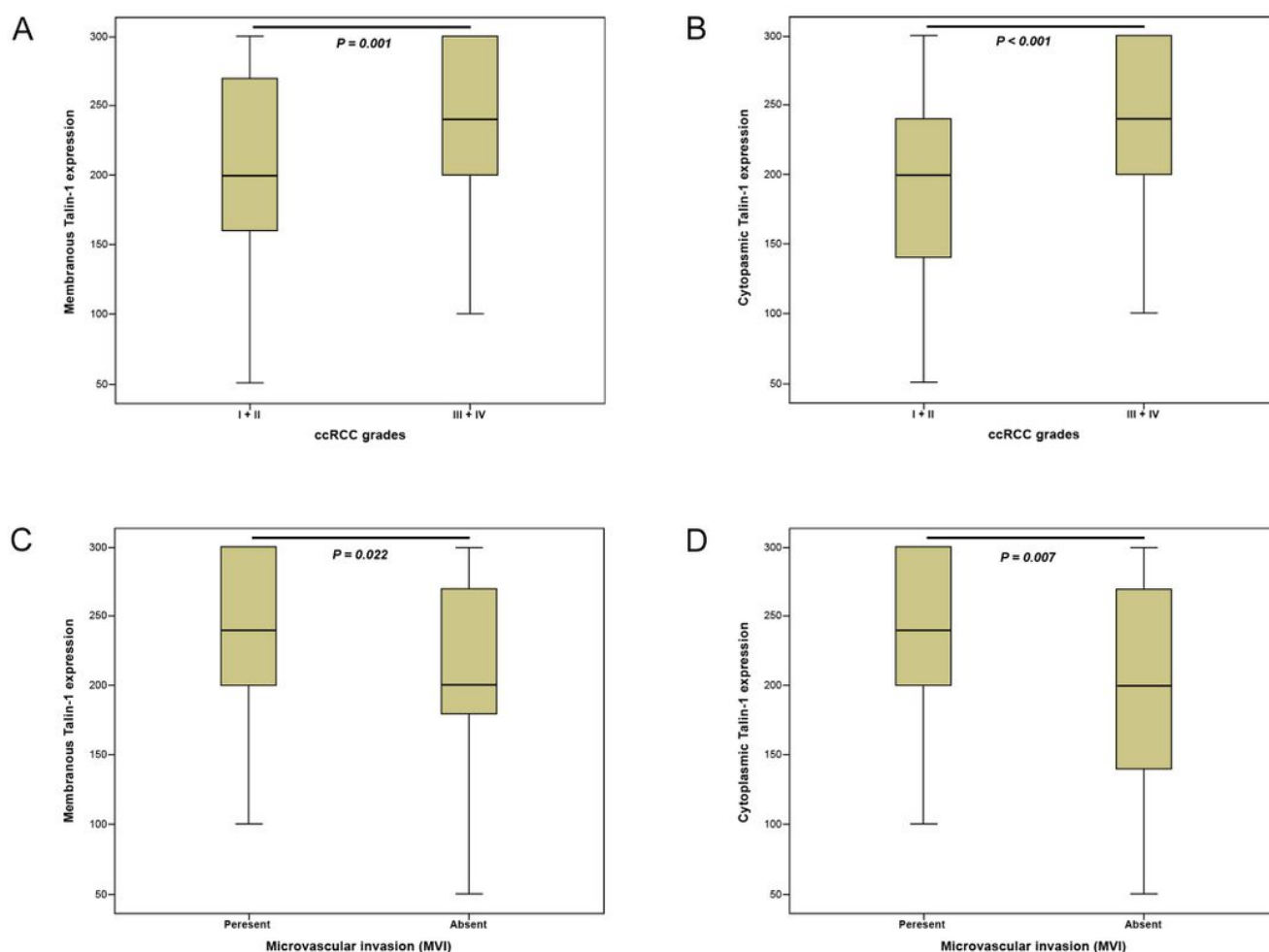


Figure 7

Box plot analysis of membranous and cytoplasmic Talin-1 protein expression levels in nuclear grade (I+ II) versus (III + IV) and microvascular invasion (MVI) present or absent in clear cell renal cell carcinoma (ccRCC) using Mann–Whitney U test. (A) (B) The results showed that there is the statistically significant association for a median of membranous and cytoplasmic Talin-1 protein expression between nuclear grade I+ II and nuclear grade III + IV ($P = 0.001$, $P < 0.001$, respectively), and also (C) (D) median expression levels of membranous and cytoplasmic Talin-1 protein and MVI present or absent ($P = 0.022$, $P = 0.007$, respectively). Based on the standard definitions, each box-plot shows the median (bold line) and interquartile lines (box).

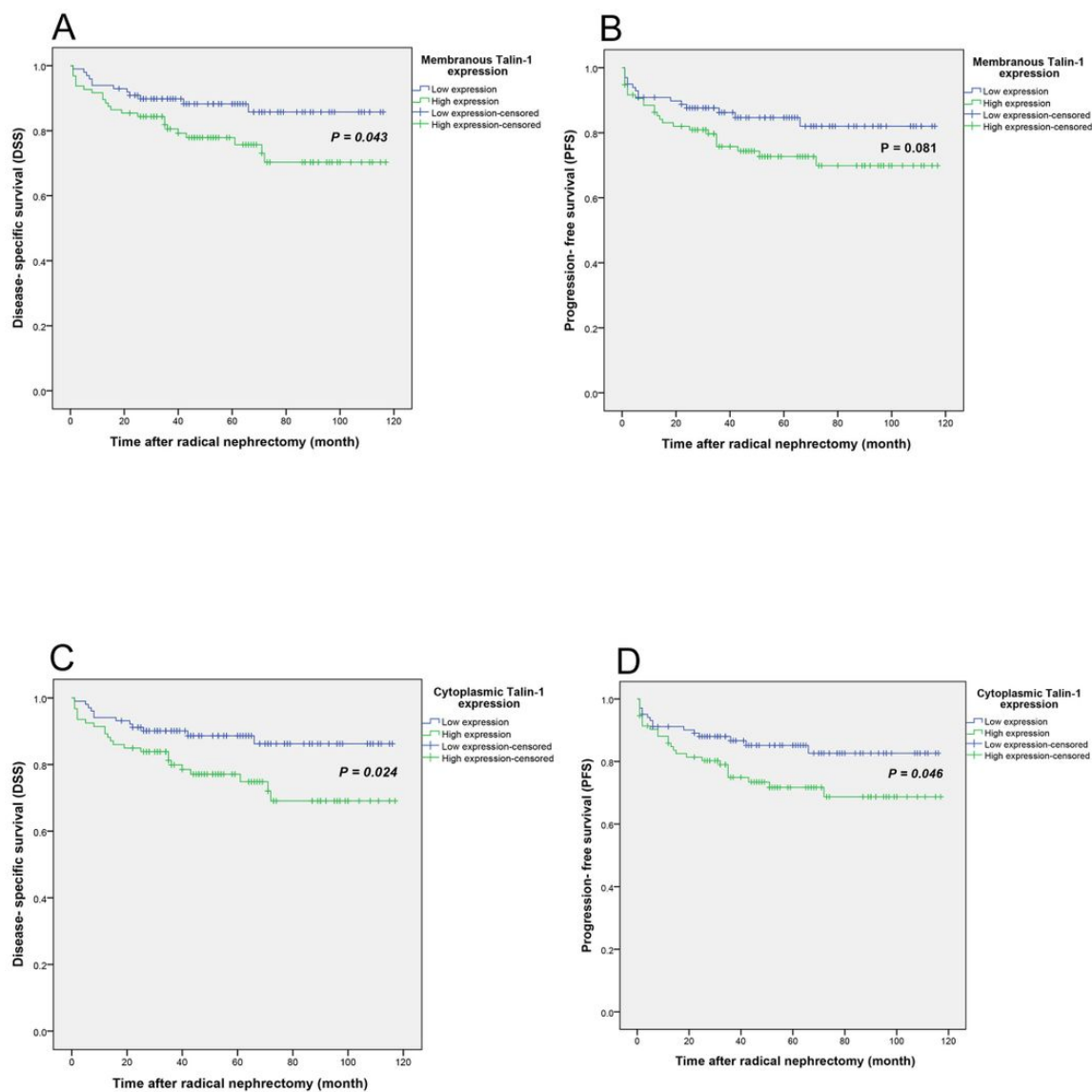


Figure 8

Kaplan–Meier curves for disease-specific survival (DSS) and progression-free survival (PFS) based on membranous and cytoplasmic Talin-1 protein expression levels in clear cell renal cell carcinoma (ccRCC). (A) In ccRCC, a higher level of membranous Talin-1 protein expression was associated with shorter DSS compared to the tumors with low expression of this protein (Log-rank test; $P = 0.043$). (B) Kaplan–Meier survival analysis showed that a high level of membranous Talin-1 protein expression is not significantly related to PFS (Log-rank test; $P = 0.081$). (C) The results showed that patients with high cytoplasmic Talin-1 protein expression have shorter DSS (Log-rank test; $P = 0.024$) or PFS (Log-rank test; $P = 0.046$) (D) compared to patients with low cytoplasmic Talin-1 protein expression.

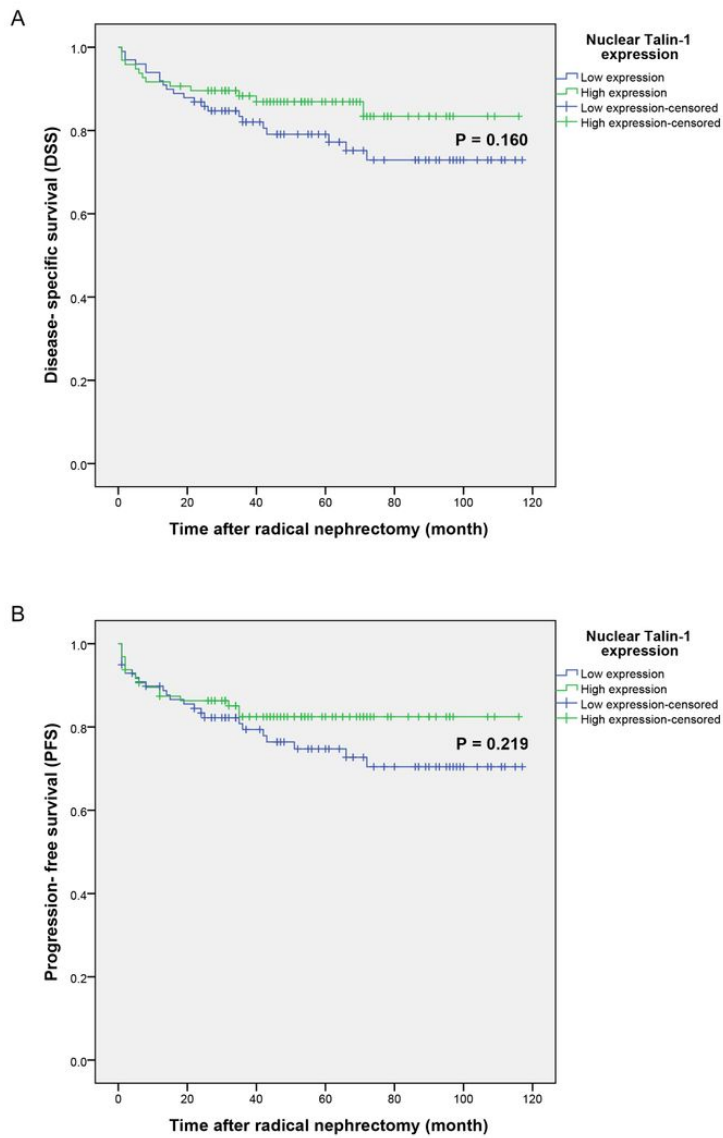


Figure 9

Kaplan–Meier curves for disease-specific survival (DSS) and progression-free survival (PFS) based on nuclear Talin-1 protein expression levels in clear cell renal cell carcinoma (ccRCC). The results showed there are no significant differences between DSS (A) or PFS (B) and the patients with high and low nuclear expression of Talin-1 protein (Log-rank test; $P = 0.160$, $P = 0.219$, respectively).

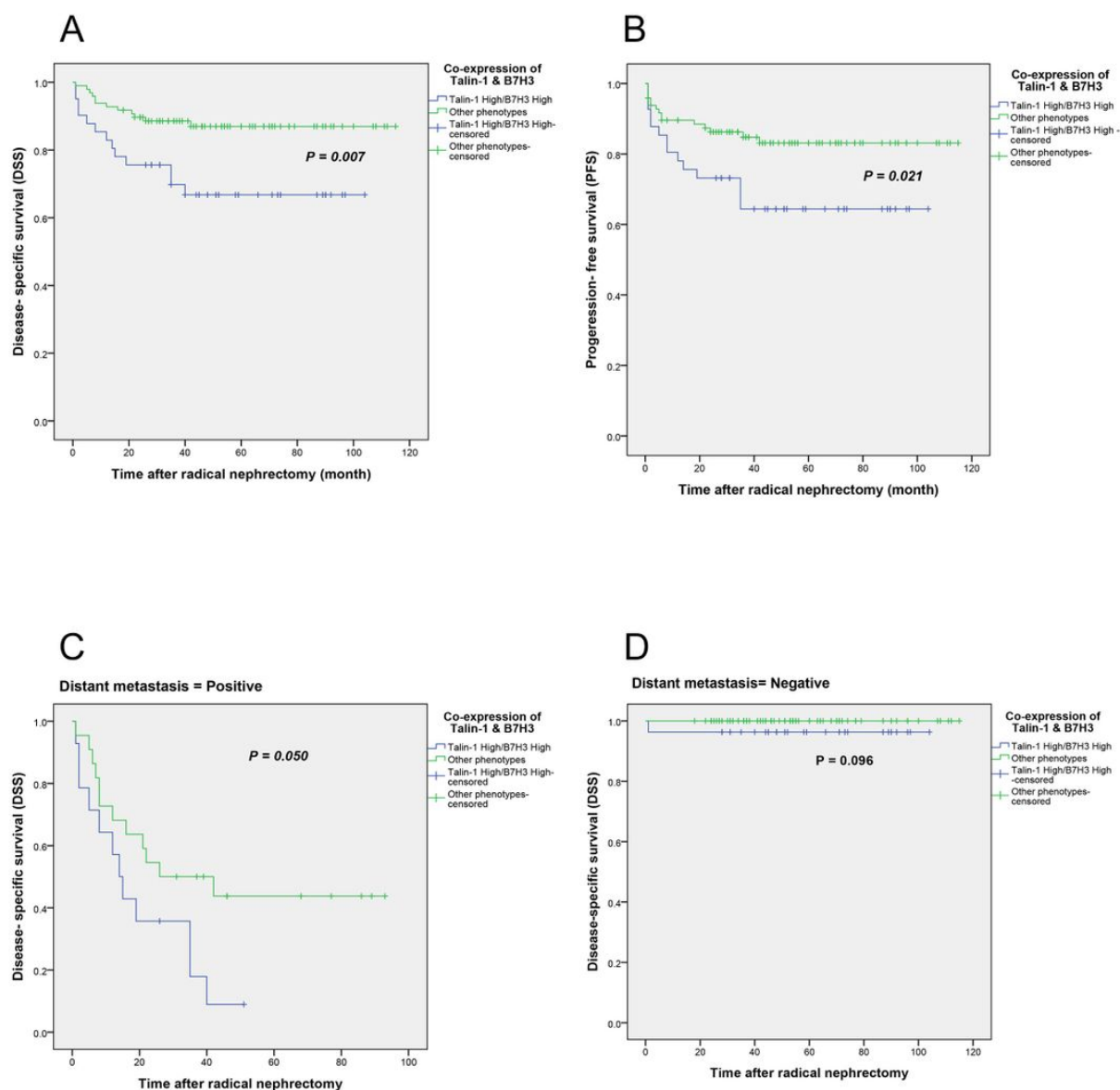


Figure 10

Kaplan–Meier curves for disease-specific survival (DSS) and progression-free survival (PFS) based on co-expression of Talin-1 and B7-H3 and stratified analysis curves of DSS for patients with distant metastasis (positive and negative) in clear cell renal cell carcinoma (ccRCC). (A) The results showed that patients with high cytoplasmic Talin-1 High/B7-H3 High protein expression have shorter DSS (Log-rank test; $P = 0.007$) or PFS (Log-rank test; $P = 0.021$) (B) compared to patients with other phenotypes of Talin-1 and B7-H3 protein expressions. (C) Stratified analysis indicated that the differences in DSS between patients with cytoplasmic Talin-1 High/B7-H3 High phenotype and other phenotypes of Talin-1/B7-H3 expression are significant ($P = 0.050$) in the patients with distant metastasis (positive) (D) but not in the negative cases. P values were calculated using the log-rank test.

Supplementary Files

This is a list of supplementary files associated with this preprint. Click to download.

- [SupplementaryFig.1.jpg](#)
- [SupplementaryTable1.xlsx](#)